2013-07-03

The Role of Nuclear BMP2 in the Cell Cycle and Tumorigenesis

Brandt Alan Nichols
Brigham Young University - Provo

The Role of Nuclear BMP2 in the Cell Cycle and Tumorigenesis

Brandt Alan Nichols

A thesis submitted to the faculty of
Brigham Young University
in partial fulfillment of the requirements for the degree of

Master of Science

Laura C. Bridgewater, Chair
Joel S. Griffitts
Julianne H. Grose

Department of Microbiology and Molecular Biology

Brigham Young University

July 2013

ABSTRACT

The Role of Nuclear BMP2 in the Cell Cycle and Tumorigenesis

Brandt Alan Nichols
Department of Microbiology and Molecular Biology
Master of Science

Bone morphogenetic protein 2 (BMP2) is a secreted growth factor that is essential for proper embryonic development and proliferation. Our laboratory discovered a nuclear variant of BMP2 (nBMP2) which is produced when translation is initiated at an alternative start codon within the BMP2 gene. When translation occurs at the downstream start codon, the resulting protein lacks the ER signal peptide, thereby allowing cytoplasmic translation and nuclear localization. Our aim is to distinguish the role of this nuclear localized variant from secreted BMP2. Overexpression of nBMP2 in HEK293 and HT29 cell lines resulted in a higher percentage of cells in proliferative phases of the cell cycle. We determined that nBMP2 does not regulate cell cycle progression by inducing hyperphosphorylation of retinoblastoma protein (Rb), but it may regulate the cell cycle by interacting with ROC1. In order to examine the role of nBMP2 *in vivo*, we have generated a mouse model in which a mutation of the nuclear localization signal (NLS) disrupts nuclear localization of nBMP2. Aberrant crypts were more abundant in nBmp2NLS^{tm} azoxymethane (AOM) treated mice than in wild type mice. Furthermore, H&E staining of colonic tissue showed that mutant mice have increased levels of dysplasia and aberrant crypt foci. This work suggests that nBMP2 is involved in regulating cell cycle progression and proliferation, and therefore may play a role in tumorigenesis.

Keywords: growth factors, nuclear localization, cell cycle, colon cancer, tumorigenesis, BMP2.

ACKNOWLEDGMENTS

I'd like to thank Dr. Laura Bridgewater for giving me the opportunity to work in her lab these past two years. She has been an ideal mentor who provided opportunities for me to present at multiple science conferences and supported me in my career aspirations. I acknowledge my committee members, Dr. Julianne Grose and Dr. Joel Griffitts, who have given me valuable advice on my project whenever I turned to them for help. I also want to thank fellow graduate student, Daniel Olsen, who has been a great friend and support over the past two years. I owe thanks to another friend and lab member, Wes Goar, who assisted greatly with the tumorigenesis experiments. Lastly, I'd like to thank my parents for their constant support in helping me be successful.

Table of Contents

List of Tables

List of Figures

Introduction

Nuclear localized BMP2

Bone Morphogenetic Protein-2 (BMP2) is a well characterized member of the transforming growth factor β (TGF-β) superfamily, named for its ability to induce bone formation [1]. In addition to its role in osteogenesis, BMP2 signaling is involved in multiple general and vital cellular processes such as proliferation and embryonic development. For example, BMP2 is essential for chondrocyte proliferation and maturation during endochondral bone development [2]. It also essential for proper embryonic development; BMP2 knockout mice are embryonic lethal since BMP2 is required for normal amnion/chorion and heart development [3].

Studies have established a correlation between BMP2 expression and cancers such as human lung carcinoma [4], breast cancer [5], and human myeloma [6]. BMP2 has been shown to suppress breast tumor growth by causing G1 arrest and promoting apoptosis [7]. BMP2 has also been shown to suppress renal tumor formation by causing G1 arrest [8]. In contrast, BMP2 promotes the migration and invasion of breast cancer cells [9]. Because of BMP2's influential roles in numerous cancer pathways, new methods of cancer treatment using this growth factor are currently being explored [10].

Although the secreted form of BMP2 has been well studied, our laboratory recently discovered a nuclear localized variant of BMP2, namely nBMP2, which avoids the secretory pathway and localizes to the nucleus after cytosolic translation [11]. Both the secreted and nuclear localized forms are transcribed from the BMP2 gene, but nBMP2 is produced when translation is initiated at a downstream alternative start codon. As secreted BMP2 is being translated, an N-terminal ER peptide signal targets the protein to the endoplasmic reticulum (ER)

and golgi to be processed by furin, which cleaves the propeptide from the mature peptide. However, when translation occurs at the alternative downstream start site, nBMP2 is translated in the cytoplasm and a bipartite nuclear localization signal that overlaps the junction between the propeptide and mature peptide directs nuclear localization (Figure 1).

nBmp2NLS^{tm} mouse model

Knock out mouse models are useful for studying the function of a specific gene. nBMP2 is transcribed from the same gene as secreted BMP2, but we generated a mutant mouse model which prevents nuclear localization of nBMP2 while allowing secreted BMP2 to be translated and processed normally. This mouse model allows us to study the unique function of nBMP2 separately from the function of secreted BMP2. Experiments have shown that there are no significant differences in skeletal structure between mutant and wild type mice suggesting that secreted BMP2 functions normally in our mouse model (unpublished data).

In order to generate a mouse model that prevents nuclear localization of nBMP2, a targeting vector was designed to introduce a mutation into the bipartite nuclear localization signal (NLS) of nBMP2; the amino acids RKR of the NLS were mutated to AAA. Mouse embryonic stem cells that successfully took up the mutation were selected for, implanted into a host embryo, and transferred to a surrogate mother (Figure 2). The heterozygous mice were bred to homozygosity and mice with the knock-in mutation are referred to as nBmp2NLS^{tm} mice.

nBmp2NLS^{tm} mice are not embryonic lethal, but unique phenotypes have been observed. In our laboratory, mice were subjected to muscle relaxation kinetics tests in which relaxation time was measured following an electrical stimulation of the muscle *in situ*. The stimulation triggers a contraction causing calcium to rush out of the sarcoplasmic reticulum (SR); following the contraction, cells pump calcium back into the SR to allow muscle relaxation. The

sarco/endoplasmic reticulum calicum ATPase 1 (SERCA1) calcium pump is embedded in the SR within muscle cells and transports calcium from the cytosol of the cell back into the lumen of the SR during muscle relaxation and studies have shown that mutations of SERCA1 negatively impact skeletal muscle relaxation [12, 13]. nBmp2NLS^{tm} mice displayed abnormalities in muscle relaxation compared to the control; half-relaxation times were prolonged up to 42% in nBmp2NLS^{tm} mice compared to wild type mice. A possible explanation for this phenotype may be explained by a decrease in SERCA1 activity since SERCA1 activity levels were determined to be 20% lower in nBmp2NLS^{tm} mice than in wild type mice (unpublished data). Decreased muscle relaxation times in nBmp2NLS^{tm} mice could be explained if nBMP2 is necessary for proper SERCA1 activity; in the absence of nBMP2 we suspect that calcium is not pumped effectively from the cytosol back into the lumen of the SR during muscle relaxation.

Further evidence suggesting nBMP2 is involved in calcium handling was observed in nBmp2NLS^{tm} mice following neurological tests. The Morris water maze test was used to assess spatial learning and memory capabilities of mice. When subjected to the Morris water maze, nBmp2NLS^{tm} mice had significantly longer escape times, approximately three times longer than escape times for wild type mice. This suggests that nBmp2NLS^{tm} mice were not able to remember and utilize visual cues for quicker escape. Furthermore, nBmp2NLS^{tm} mice displayed memory deficits during novel object recognition tests. nBmp2NLS^{tm} mice spent significantly less time exploring novel objects within their cage compared to wild type mice. This suggests mutant mice have multiple neurological deficits in pathways that depend on proper calcium signaling.

Memory deficits of nBmp2NLS^{tm} mice were quantified by measuring long-term potentiation (LTP). LTP is described as a long-lasting enhancement in transmission signal

between two neurons. These signals are measured in the hippocampus, an organ of the brain important for learning and memory. LTP experiments using hippocampal tissue showed that LTP levels were significantly lower in nBmp2NLS^{tm} mice than in wild type mice (unpublished data). LTP is considered one of the major cellular mechanisms associated with memory and learning, and one of the mechanisms associated with synaptic plasticity. Synaptic plasticity is the ability for connection between two neurons to change in strength, and studies show that calcium signaling is an important part of synaptic plasticity [14, 15]. LTP is dependent on proper calcium signaling between neurons in the brain [16, 17]. For example, IP3-dependent calcium release has been shown to be a mechanism for trans-synaptic mechanisms that regulate LTP in rat ganglion [18]. It is possible that calcium dysregulation may explain the memory deficits of nBmp2NLS^{tm} mice since impaired calcium handling would decrease the synaptic plasticity between neurons.

Both the skeletal muscle and memory impairment phenotypes suggest that nBmp2NLS^{tm} mice have abnormal calcium handling. Therefore it is likely that nBMP2 is involved in regulating calcium channels since mice display deficits in muscle and neurological tissue which are highly dependent upon calcium signaling for normal function.

Cell cycle regulation

Calcium handling is not only important for signaling in muscle and neurological systems, but also plays an important role in cell signaling pathways that control cell proliferation. Calcium is important for signaling in cell cycle transitions, as observed by cystolic calcium levels peaking at the G_1/S checkpoint and steadily decreasing through S-phase [19]. Because our nBmp2NLS^{tm} mice display abnormalities in calcium handling, we hypothesized that nBMP2 may be involved in regulating the cell cycle progression at cell cycle checkpoints.

Cell cycle regulation is normally kept within tight control to prevent unwarranted cellular proliferation. One of the major and well-studied guardians of the cell cycle is retinoblastoma protein (Rb), which prevents cell cycle progression at the checkpoint between G_1/S phases [20, 21]. When cyclin dependent kinases (CDKs) are present, they hyperphosphorylate Rb, prevent its inhibitory actions, and allow entry from resting phases of the cell cycle into S-phase [22]. Measuring phosphorylation of Rb is a common and useful method for determining whether cells are undergoing cell proliferation by overcoming the G_1/S phase checkpoint.

In order for CDKs to be able to phosphorylate Rb and cause cell cycle progression, cyclin dependent kinase inhibitors (CKIs) must be degraded [23]. The SCF ubiquitin ligase complexes are important for targeting CKIs for degradation, thus allowing cell cycle progression [24]. A yeast two-hybrid interaction between nBMP2 and Regulator of Cullins (ROC1, also known as RBX-1) was demonstrated (Bridgewater lab, unpublished data). ROC1 is a member of the SCF E3 ubiquitin ligase complex, which is responsible for targeting several different cell cycle inhibitors for degradation so that the cell cycle can proceed and is important for cancer cell survival [25]. We seek to verify the interaction between nBMP2 and ROC1 because nBMP2 may drive cell cycle progression by interacting with ROC1 of the SCF-E3 ubiquitin ligase complex to facilitate degradation of cell cycle inhibitors.

Uncontrolled cellular proliferation is a hallmark of cancer, often a result of mutations in proteins that serve to regulate cell cycle progression [26]. Abnormalities in calcium meditated signaling pathways are characteristic of cancers and facilitate tumor progression, cell proliferation, metastasis, and invasion [27]. Because nBmp2NLS^{tm} mice display abnormalities in calcium handling, we hypothesized that nBMP2 may also be involved in tumorigenesis. A microarray analysis performed in our laboratory performed showed an association between

overexpression of nBMP2 and increased transcription of sarcoplasmic endoreticulum Ca^{2+} ATPase 2 (SERCA2), and SERCA2 mRNA levels have been demonstrated to be upregulated in colorectal cancer [28]. Therefore, colorectal cancer is a good candidate to study the involvement of nBMP2 in tumorigenesis. Furthermore, we've been able to visualize endogenous expression of nBMP2 in a colorectal cancer cell line (HT29) and numerous other cancer cell lines (MCF-7, Hep-G2, MDA-MB-231, MDA-MB-435) suggesting it may function as an oncoprotein (Figure 3).

Thus far, no one has separated the roles of recently discovered nBMP2 from that of secreted BMP2, both derived from the same gene and transcript. Work in our laboratory suggests that nBmp2NLS^{tm} mice are viable but display abnormalities in calcium handling. Abnormalities in calcium handling are characterized in many cancers, and calcium handling is important in signaling for cell proliferation. Because nBMP2 appears to be required for normal calcium handling, we hypothesize that nBMP2 interacts with calcium channel regulatory proteins that are involved in regulating proliferation and tumorigenesis. In this study we provide evidence that nBMP2 does indeed regulate cell cycle progression and tumorigenesis.

Materials and Methods

Plasmid constructs

Myc-tagged nBMP2 constructs were created according to the protocol provided with the QuickChange II Site-Directed Mutagenesis Kit (Stratagene, La Jolla, CA). Myc tags were incorporated onto either the N or C terminus of the nBMP2 sequence. Primers were designed to incorporate the tag into an nBMP2-pcDNA3.1(+) plasmid construct (Table 1). In order to confirm nBMP2 was effectively tagged, plasmids were transiently transfected into HEK293 cells and protein lysate was analyzed by western blot and probed with Myc-tag antibody (Cell Signaling, Cat. No. 2278). The plasmid constructs are referred to as nBMP2-N-MYC and nBMP2-C-MYC, N and C referring to which terminus is tagged.

FLAG-tagged PLSCR1 was also created using the QuickChange II Site-Directed Mutagenesis Kit. Primers were designed to incorporate a FLAG tag onto the N-terminus of PLSCR1into a PLSCR1-pcDNA3 construct (generously provided by Peter J. Sims, University of Rochester) (Table 1). In order to confirm PLSCR1 was effectively tagged, the plasmid construct was transiently transfected into HEK293 cells and protein lysate was analyzed by western blot by probing with FLAG antibody (Cell Signaling, Cat. No. 8146). The plasmid construct is referred to as PLSCR1-N-FLAG.

A plasmid construct for HA-tagged ROC1 was generously donated by Dr. Yi Sun of University of Michigan and is referred to as ROC1-HA.

In order to express nBMP2 and GFP separately using the same expression vector, we cloned nBMP2 into pBigT-IRES-GFP (pBTG) using SalI and ClaI. The pBTG plasmid was used as a control since it contains the IRES-GFP sequence and produces GFP only.

We also made a construct with nBMP2 fused to a GFP reporter. nBMP2 in pcDNA3.1(+) was used as a template for the production of the nBMP2-GFP fusion construct using a GFP Fusion TOPO TA Expression Kit (Invitrogen Corporation, Carlsbad, CA) according to the manufacturer's instructions [29]. This construct has GFP fused to the C-terminus of nBMP2 and is referred to as nBMP2-C-GFP.

Transient Transfection

HEK293 cells were cultured at 37°C, 5% CO2 in a 50:50 mix of Dulbecco's Modified Eagle Medium and Ham's F-12 media (DMEM/F12) (Cellgro, Corning, NY) supplemented with 10% FBS and L-glutamine. HEK293 cells were transfected by seeding 600,000 cells into each well of a 6-well cell culture plate on day one. On day two, cells were transiently transfected using Lipofectamine 2000 (Lipo 2000) (Invitrogen, Carlsbad, CA) by adding 4 µg of DNA and 10 µl Lipo 2000 to 250 µl Opti-MEM® I Reduced Serum Media (Opti-MEM) (Life Technologies, Carlsbad, CA). The DNA/Opti-MEM/Lipo 2000 mixture was incubated at RT for 20 min and then added to drop-wise to each well. 48 hours post transfection, cells were harvested for analysis.

HT29 cells were cultured at 37°C, 5% CO2 in RPMI-1640 media (RPMI) (Sigma Aldrich, St. Louis, MO) supplemented with 10% FBS and L-glutamine. HT29 cells were transfected by seeding 750,000 cells into each well of a 6-well cell culture plate on day one. The following day, cells were transiently transfected by adding 4 µg of DNA and 25 µl Lipo 2000 to 250 µl Opti-MEM. The DNA/Opti-MEM/Lipo 2000 mixture was incubated in a microcentrifuge tube at RT for 20 min and afterwards 4 µl of MA Lipofection Enhancer (IBA, Goettingen, Germany) was added to each tube. The mixtures incubated at RT for 15 min. Media was then removed from the each well of the 6-well plate and 1.5 ml of 37°C pre-heated Opti-

MEM was added to each well. The mixture was then added to cells drop-wise and immediately placed on a magnetic plate for 15 minutes. Cells were removed from the magnetic plate and incubated for 5 hours at 37°C, 5% CO2. After the 5 hour incubation period, media was replaced in each well with 2 ml of fresh, supplemented RPMI. 48 hours post transfection, cells were harvested for analysis.

Western Blots

Protein concentration was determined using the Bradford Assay using Protein Assay Dye Reagent Concentrate (Biorad, Hercules, CA). Protein lysate samples were separated by a 10% tris-glycine sodium dodecyl sulfate polyacrylamide gel electrophoresis (SDS-PAGE) and transferred to nitrocellulose membranes. The membranes were then probed with primary antibody at a proper dilution in non-fat dry milk (NFDM) for 22 hours at 4°C. Afterwards, membranes were washed and probed with anti-rabbit IgG HRP-linked secondary antibody (Cell Signaling, Cat. No. 7074) or anti-mouse IgG HRP-linked secondary antibody (Cell Signaling, Cat. No. 7076) for 60 minutes at RT in NFDM. Membranes were then incubated with Immobilon™ Western Chemiluminescent HRP Substrate (Millipore, Billerica, MA) for 5 minutes at RT and exposed by autoradiography onto Blue Basic Autorad Film (ISC Bioexpress, Kaysville, UT).

Cell cycle analysis

For both HEK293 and HT29 cell lines, three wells of a 6-well plate were transiently transfected with a GFP control vector and the other three wells were transiently transfected with a plasmid construct which constitutively and separately expresses nBMP2 and GFP, namely nBMP2-IRES-GFP.

48 hours post transient transfection, cells were washed with PBS and then suspended in 500 µl of fresh PBS by pipetting the cells into a single-cell suspension. Cells were transferred to a 5 ml tube and fixed by incubating with 500 µl of ice cold 2% formaldehyde (methanol-free) for 10 min at 4°C. The mixture was then spun in a swinging-bucket centrifuge at 1500 rpm at 4°C for 5 min. After removing the supernatant by gentle aspiration, cells were washed once with 1 ml of cold PBS and spun again under same conditions for 5 min. To permeabilize the cells, the PBS supernatant was removed and 1 ml of cold 70% ethanol was added drop-wise to the cell pellet while the tube was gently vortexed. The cell suspension was incubated overnight at 4°C.

Following overnight incubation, cells were centrifuged for 5 min at 1500 rpm at 4°C, supernatant was gently aspirated, the pellet washed with 1 ml of PBS, and then centrifuged again for 5 min at 1500 rpm. Following removal of supernatant, the cell pellet was suspended in 1 ml of propidium iodide (PI) staining solution (10 µg/ml PI and 100 µg/ml DNase-free RNase A, diluted in PBS) (Life Technologies, Carlsbad, CA). Cells were kept in the dark at RT for 30 min before analysis by flow cytometry (FACSCanto, BD Biosciences, BYU RIC facility). GFP positive cells were gated and cell cycle analysis was performed using Modfit LT software (Verity Software House). Each experiment was replicated three times and data were averaged before statistical analysis by an unpaired t-test.

MG132 experiment

On day one, HEK293 cells were transiently transfected with nBMP2-N-MYC. 36 hours post transfection, 10 µM MG-132 (Sigma Aldrich, St. Louis, MO) was added to some wells to inhibit proteasome activity. 12 hours after addition of MG-132, cells were lysed with NP-40 lysis buffer [50 mM Tris-HCl (pH 7.5), 150 mM NaCl, 0.5% NP-40, 50 mM NaF, 1 mM Na_3VO_4, 1 mM DTT, 1x Pierce Protease Inhibitor Cocktail (Fisher Scientific, Pittsburgh, PA),

and 1 mM phenylmethanesulfonyl fluoride (PMSF)]. To prepare lysate for analysis by SDS-PAGE, 30 µl of protein lysate was added to 10µl of 4X loading buffer, boiled for 5 minutes, and then stored at 4°C.

Protein concentration was determined using the Bradford Assay and 30 µg samples were separated by a 10% tris-glycine SDS-PAGE and transferred to nitrocellulose membranes. The membranes were probed with anti-Myc primary antibody (Cell Signaling, Cat. No. 2278) at a 1:1000 dilution for 22 hours at 4°C. The membranes were washed and probed with anti-rabbit IgG HRP-linked secondary antibody (Cell Signaling, Cat. No. 7074) at a 1:2000 dilution for 60 minutes at RT.

Rb western blot analysis

Three wells of a 6-well plate were transiently transfected with nBMP2-IRES-GFP, and the other three wells with GFP control plasmid. 48 hours after transfection, cells were lysed with NP-40 lysis buffer. Protein concentration was determined using the Bradford assay, and samples were then boiled in 4X loading buffer and stored at 4°C until separated by SDS-PAGE. Following protein transfer, nitrocellulose membranes were probed with anti-Rb primary antibody (Cell Signaling, Cat. No. 9969) or with GAPDH (Cell Signaling, Cat. No. 2118) at a 1:1000 dilution O/N at 4°C. The membranes were washed and probed with anti-rabbit IgG HRP-linked secondary antibody (Cell Signaling, Cat. No. 7074) at a 1:2000 dilution for 60 minutes at RT.

PLSCR1/nBMP2 co-immunoprecipitation experiments

To test for an interaction between nBMP2 and PLSCR1, HEK293 cells were transiently transfected with nBMP2-C-MYC, PLSCR1-N-FLAG, or with both plasmids. Samples were transfected in duplicates and combined together after lysis by NP-40 lysis buffer. To prepare lysate controls, 30 µl of protein lysate was added to 10µl of 4X loading buffer, boiled for 5 min,

and stored at 4°C until separated by SDS-PAGE. 10 µl of Myc-Tag (9B11) Mouse mAb (Sepharose Bead Conjugate) (Cell Signaling, Cat. No. 3400) was added to 200 µg of protein lysate and sample was rotated O/N at 4°C. The next day, samples were microcentrifuged at 14,000 rpm for 1 min at 4°C and washed 5 times with NP-40 cell wash buffer [50 mM Tris-HCl (pH 7.5), 150 mM NaCl, 0.5% NP-40, 50 mM NaF]. After the final wash, 30 µl 1X loading dye was added to the sepharose beads and samples were boiled for 5 minutes and stored at 4°C until separated by SDS-PAGE. For SDS-PAGE, each well was loaded with 15 µl of each lysate and pull-down sample. Membranes were blocked with NFDM and probed with either anti-Myc antibody (Cell Signaling, Cat. No. 2278) or anti-FLAG antibody (Cell Signaling,Cat. No. 2368) at a 1:1000 dilution for 22 hours at 4°C.

ROC1/nBMP2 co-immunoprecipitation experiments

To test for a protein-protein interaction between nBMP2 and ROC1, HEK293 cells were transiently transfected with nBMP2-C-MYC, ROC1-HA, or with both plasmids. Samples were transfected in duplicates and combined together after lysis by NP-40 lysis buffer. To prepare lysate controls, 30 µl of protein lysate was added to 10µl of 4X loading buffer and boiled for 5 minutes. 10 µl of Myc-Tag (9B11) Mouse mAb (Sepharose Bead Conjugate) (Cell Signaling, Cat. No. 3400) was added to 200 µg of protein lysate and sample was rotated O/N at 4°C. The next day, samples were microcentrifuged at 14,000 rpm for 1 min at 4°C and washed 5 times with NP-40 cell wash buffer. After the final wash, 30 µl 1X loading dye was added to the sepharose beads and samples were boiled for 5 minutes and stored at 4°C until separated by SDS-PAGE. Each well was loaded with 15 µl of each lysate and pull-down sample. Membranes were blocked with NFDM and probed with either anti-Myc antibody (Cell Signaling, Cat. No.

2278) at a 1:1000 dilution or anti-HA antibody (Roche, Palo Alto, CA) at a 1:2000 dilution for 22 hours at 4°C.

Azoxymethane experiments

Two different tumorigenesis studies were performed, one 6 weeks and the other 12 weeks long. In both studies, 6-8 month old male mice were given three weekly intraperitonial injections of azoxymethane (AOM) dissolved in PBS, or PBS solution only, at 10 mg/kg body weight. A total of 13 nBmp2NLS^{tm} and 10 wild type mice were used in 6-week study, while 10 nBmp2NLS^{tm} and 10 wild type mice were used in the 12-week study. Mice were weighed weekly until the day they were sacrificed. Mice were euthanized 28 or 63 days after the final injection, mouse colons were removed, fecal matter cleaned out with PBS, and each colon was cut into two 5 cm segments. The colons were cut open longitudinally and fixed flat in 70% ethanol at 4°C O/N. The next day the tissues were stained with 0.05% methylene blue for 3 min, rinsed with distilled H20, and aberrant crypts were quantified using light microscopy.

Histology

Two mouse colons from each AOM study were dissected to perform hematoxylin and eosin (H&E) staining of the colonic tissue. For each study, colons from one AOM treated mouse of each genotype were dissected either 28 or 63 days after the final injection of AOM and fixed flat in 4% paraformaldehyde overnight at 4°C. The following day, tissues were rinsed 3 times for 20 min with PBS, then 30 min in 30% EtOH, another 30 min in 50% EtOH, and then overnight in 70% EtOH at 4°C. The tissues were processed overnight in a Citadel 1000 processor and embedded in paraffin wax. Using a Microm HM 325 Rotary Microtome (Thermo Scientific, Waltham, MA) the samples were cut into 5 µm thick sections and dried onto glass slides O/N at 37°C. Slides were deparaffinized in Histo-Clear (National Diagnostics, Charlotte,

NC) and colon sections were then stained with Richard-Allan Scientific Signature Series Hematoxylin 1 and Eosin-Y (Thermo Fisher Scientific, Waltham, MA) (Table 2). Immediately after H&E staining, Vectamount Permanent Mounting Medium (Vector Laboratories, Burlingame, CA) and coverslips were applied. The stained sections were visualized and imaged by light microscopy.

Results

nBMP2 promotes cell cycle progression in HEK293 cells

We found in a yeast-two-hybrid screen that nBMP2 interacts with ROC1, a member of the SCF E3 ubiquitin ligase complex that targets proteins, including cell cycle inhibitors, for degradation. In order to determine whether nBMP2 affects cell cycle progression, we overexpressed nBMP2 in HEK293 cells and compared cell cycle distribution to that of a control.

Cell cycle analysis software showed that nBMP2 overexpression resulted in a higher percentage of cells in S-phase of the cell cycle compared to the control (Figure 4). In HEK293 cells, nBMP2 overexpression caused the amount of cells in resting phases (G0/G1) to decrease from 56% to 47% and the percentage of cells in proliferative phases (S/G2) to increase from 44% to 53% (Figure 5). These data suggest that nBMP2 is involved in regulating cell cycle progression in HEK293 cells *in vitro*.

nBMP2 promotes cell cycle progression in colorectal cancer HT29 cells

A prior microarray analysis showed that the ER calcium pump SERCA2 was upregulated in response to nBMP2 overexpression. Because SERCA2 upregulation is a characteristic observed in colorectal cancers [28], we tested whether nBMP2 would drive cell cycle progression in an HT29 colorectal cancer cell line. We overexpressed nBMP2 in HT29 cells and compared cell cycle distribution to that of a control.

Similar to results obtained in HEK293 cells, nBMP2 overexpression caused the amount of cells in resting phases (G0/G1) to decrease from 46% to 36% and the percentage of cells in proliferative phases (S/G2) to increase from 54% to 64% (Figure 6). These data suggest that

nBMP2 is indeed involved in regulating cell cycle progression in a colorectal cancer cell line *in vitro*.

nBMP2 is actively degraded by the proteasome

Having shown that nBMP2 affects cell cycle regulation, we conducted these experiments to test whether it is actively degraded by the proteasome as are many other cell cycle regulatory proteins. When MG-132 proteasome inhibitor was added to cells transfected with nBMP2-N-MYC, higher levels of non-degraded nBMP2 accumulated and were observed on a western blot (Figure 7). This indicates that nBMP2 is actively degraded by the proteasome.

Rb is not hyperphosphorylated with nBMP2 overexpression

Overexpression of nBMP2 increases the percentage of cells in proliferative phases of the cell cycle. Phosphorylation of Rb is one of the main mechanisms that regulates the checkpoint between G1 and S phases of the cell cycle; Rb must be hyperphosphorylated at sites including Ser 807, Ser 811, Ser 795, and Ser 780 in order to temporarily remove its inhibitory effects on the G1/S checkpoint. Therefore, we performed western blots to determine whether overexpression of nBMP2 leads to hyperphosphorylation of Rb. Most Rb phosphorylation sites were unaffected by nBMP2 overexpression (Figure 8). However, our initial experiment suggested more phosphorylation at the Rb Ser780 site with nBMP2 overexpression compared to the control.

After repeating this experiment for Rb Ser780 using triplicate samples, we determined that there is no significant increase in the amount of phosphorylation at this site for nBMP2 overexpression compared to the control (Figure 9). We conclude that nBMP2 does not drive cell cycle progression by inducing hyperphosphorylation of Rb.

C-terminal nBMP2 fusion protein also promotes cell cycle progression

Because we wanted to use tagged versions of nBMP2 in subsequent experiments, we tested whether a C-terminally fused tag would inhibit nBMP2's effect on the cell cycle. In order to test this, HEK293 cells were transiently transfected with the nBMP2/GFP fusion construct, nBMP2-C-GFP, and compared to a GFP control using cell cycle analysis as previously described. Even with GFP fused to the C-terminus, nBMP2-C-GFP was still able to drive cell cycle progression. The percentage of cells in G0/G1 phases decreased from 58% to 42% and the percentage of cells in S/G2 phases increased from 34% to 56% (Figure 10). These data indicate that a GFP protein tag fused to the C-terminus of nBMP2 does not interfere with any interactions that are necessary for nBMP2 to affect the cell cycle, giving us confidence to proceed with using C-tagged nBMP2 in co-immunoprecipitation experiments.

Protein-protein interaction of nBMP2 with PLSCR1

A yeast 2-hybrid screen suggested a protein-protein interaction between nBMP2 and PLSCR1, a protein shown to upregulate expression of inositol trisphosphate receptor type 1 (IP3R1), a protein involved in regulating the release of calcium from endoplasmic reticulum [30]. Verifying this interaction is important to determine whether nBMP2 regulates calcium handling by regulating expression of the IP3R1 calcium channel by interacting with PLSCR1. We performed co-immunoprecipitation experiments on cells transfected with nBMP2-N-MYC or nBMP2-C-MYC and PLSCR1-N-MYC and immunoprecipitated with anti-Myc or anti-FLAG antibody. Immunoprecipitation with anti-Myc antibody did not show an interaction of PLSCR1 with either C or N terminally tagged nBMP2, even after a 45 min exposure (Figure 11). Immunoprecipitation with anti-FLAG antibody did not give decipherable results due to excessive background (data not shown).

Protein-protein interaction of nBMP2 with ROC1

A yeast 2-hybrid screen suggested that nBMP2 interacts with ROC1, a member of the SCF-E3 ubiquitin ligase complex, which tags cell cycle inhibitors for degradation. nBMP2 could regulate cell cycle progression by interacting with ROC1 of the SCF-E3 ubiquitin ligase complex to facilitate degradation of cell cycle inhibitors. In order to verify an interaction between nBMP2 and ROC1, we performed co-immunoprecipitation experiments by transfecting cells with nBMP2-N-MYC or nBMP2-C-MYC and ROC1-HA and immunoprecipitated with anti-Myc or anti-HA antibody. Although immunoprecipitation with anti-Myc antibody shows there may be an interaction between ROC1 and nBMP2, this interaction needs to be further verified due to non-specific binding of ROC1-HA to Myc-sepharose beads (Figure 12). Immunoprecipitation with anti-HA antibody did not give decipherable results due to excessive background (data not shown).

nBmp2NLS^{tm} mice display more aberrant crypt formation and dysplasia in colon

Because nBMP2 promotes cell cycle progression in the HT29 colon cancer cell line, we tested whether nBMP2 is involved in tumorigenesis *in vivo* by inducing colon cancer in the nBmp2NLS^{tm} mouse model using azoxymethane (AOM).

In the 6-week study, there were measureable but insignificant differences in weights between AOM treated mutant and wild type mice from days 15 to 43; nBmp2NLS^{tm} had a greater decrease in percent of original body weight compared to wild type mice (Figure 13). Mice injected with AOM developed quantifiable aberrant crypts (Figure 14A). However, no significant differences in the number of aberrant crypts were observed between nBmp2NLS^{tm} mice and wild type mice after 6 weeks (Figure 14). However, H&E staining of longitudinal colon tissue sections revealed increased levels of dysplasia and increased number of nuclei in

nBmp2NLS^{tm} mice compared to wild type mice (Figure 15). Therefore, we conclude that the absence of nBMP2 may result in increased tumorigenesis when cancer is induced.

In the 12-week study, there were no significant changes in percent of original body weight between nBMP2NLS^{tm} and wild type mice injected with AOM (Figure 16). However, on average there were more aberrant crypts observed in AOM treated nBmp2NLS^{tm} mice compared to wild type mice (Figure 17). No aberrant crypts were observed in the PBS control mice. In addition, aberrant crypts were more frequently observed in AOM treated nBmp2NLS^{tm} than wild type mice in H&E stained longitudinal sections of colon tissue (Figure 18). From the 12-week study we conclude that with increased time there is a greater difference in tumorigenesis between nBmp2NLS^{tm} and wild type mice and that lack of nBMP2 results in increased aberrant crypt formation.

Discussion

Nuclear variants of growth factors regulate cell proliferation

Nuclear localized variants of growth factors are less studied than their secreted counterparts, but several have been shown to regulate cell proliferation. For example, nuclear localized PtHRP increases cell growth and survival, and protects cells from serum-starvation-induced apoptosis via an intracine pathway [31]. Nuclear localized FGF-2 is also involved in regulation of cell proliferation, specifically by stimulating the phosphorylation of nucleonin by CK2 [32]. Nuclear localization of FGF-3 is similar to that for nBMP2; alternative translation begins at an upstream start codon and incorporates a nuclear localization signal. FGF-3 nuclear and secreted forms have opposite functions; the secreted form induces proliferation while the nuclear localized form down-regulates proliferation [33]. If nBMP2 functions in a similar manner to FGF-3, this suggests that nBMP2 and BMP2 may balance each other's effects on cell proliferation in a similar manner to the nuclear and secreted forms of FGF-3.

The molecular mechanism of nBMP2 in tumorigenesis

nBMP2 was discovered by DNA affinity chromatography when fragments of BMP2 proprotein were recruited to a DNA enhancer element that was known to bind the transcription factor SOX9 [11]. The relationship between SOX9 and nBMP2 has been explored, but thus far we haven't been able to determine that these two proteins interact. Interestingly, an alternative version of SOX9, named Mini-SOX9, was discovered to play a role in colon cancer development [34]. Mini-SOX9 is not generated by alternative translation like nBMP2, but rather by alternative mRNA splicing. Mini-SOX9 is a truncated version of SOX9 that localizes to the nucleus and is upregulated in colon cancer tissues but not in surrounding healthy tissue. We

suspect that nBMP2 is also upregulated in cancer tissues since it has been observed in several cancer cell lines, but has not yet been observed in primary cells.

Mini-SOX9 activates the Wnt signaling pathway and promotes β-catenin nuclear localization. Although we do not yet know the binding partners of nBMP2, it may interact with proteins to activate a similar cell pathway that regulates proliferation. SOX9 has anti-oncogenic function while Mini-SOX9 has oncogenic function, and they function independently of each other. We suggest that nBMP2 could have independent oncogenic function which drives the cell cycle progression we observed *in vitro*. Several studies show that BMP2 has anti-oncogenic function [7, 8] suggesting that nBMP2 and BMP2 may have balancing effects on tumor progression similar to that for Mini-SOX9 and SOX9.

Overexpression of nBMP2 promoted cell cycle progression *in vitro*, and yet lack of nBMP2 increased levels of aberrant crypt formation *in vivo*. It will be important to determine the molecular mechanism by which nBMP2 regulates cell proliferation to determine why overexpression and absence of nBMP2 would both drive proliferation. A possible explanation for this paradox is that there are other factors involved *in vivo* that are not present *in vitro*. Another explanation is that nBMP2 levels must be carefully regulated and either too much or too little nBMP2 expression results in increased proliferation and tumorigenesis. In order to test whether nBMP2 overexpression would also increase tumorigenesis *in vivo*, a mouse model would need to be generated that overexpresses nBMP2 in the colon. Either way, nBMP2 appears to be involved in regulating cell proliferation both *in vitro* and *in vivo*.

Conclusions and future directions

We conclude that nBMP2 plays a role in the cell cycle and tumorigenesis, although the mechanism by which it does this remains to be determined. In order to determine this

mechanism, it will be important to identify the binding partners of nBMP2. To accomplish this, we will pull down nBMP2 by co-immunoprecipitation and identify binding partners by mass spectrometry. We are particularly interested in those that interacted with nBMP2 in our yeast 2-hybrid screen, including PLSCR1 and ROC1. Since apoptosis regulation is relevant to cancer development, another binding-partner candidate is apoptosis-inducing factor SIVA1, which was shown to interact with nBMP2 in the yeast 2-hybrid screen. An interaction may be verified between SOX9 and nBMP2 since nBMP2 was discovered in a DNA affinity chromatography experiment with an enhancer element that also binds SOX9. Proteins involved in regulating proliferation or calcium handling will be of most interest due to the phenotypes observed *in vitro* and in our nBmp2NLS^{tm} mouse model.

Because nBMP2 has been shown to be expressed in cancer cell lines, we will also perform immunohistochemistry on an array of human cancer tissues to examine nuclear localization of nBMP2 in cancerous tissues compared to normal tissue. We suspect that human cancer tissue will have an increased amount of nuclear staining for nBMP2.

Calcium signaling is important for many cellular processes including gene expression, cell cycle regulation, muscle contraction, neuronal synapse signaling, and immune function. Our studies suggest that nBMP2 is involved in regulating calcium handling, but the pathway by which nBMP2 regulates calcium handling is yet to be determined. It is of interest that nBMP2 is readily observed in immortalized and cancer cell lines but has not yet been observed in primary cells. This suggests that nBMP2 expression is either tissue-specific or time-specific. It is also possible that nBMP2 is only expressed under certain stress, such as when cancer is induced. Determining when and where nBMP2 is expressed will be important to determine which pathways nBMP2 is involved in and how it regulates cell cycle progression and tumorigenesis.

Tables

Table 1. Mutagenesis primers to generate Myc-tagged nBMP2 and FLAG-tagged PLSCR1
Primers were generated to incorporate a Myc tag onto both the N and C terminus of nBMP2. Primers to incorporate a FLAG tag onto the N-terminus of PLSCR1 are also listed. Yellow indicates start codon, cyan indicates glycine linker, magenta indicates stop codon, and the underlined sequence indicates the tag.

Primer name	Primer sequence
N-MYC forward primer	CCCTTAAAAAGCTGCTCAGCATGGAGCAGAAGCTGATCAGCGAGGAGGACCTGGGTGGCGGAGGTGGCTTTGGCCTGAAGCAGAGACC
N-MYC reverse primer	GGTCTCTGCTTCAGGCCAAAGCCACCTCCGCCACCCAGGTCCTCCTCGCTGATCAGCTTCTGCTCCATGCTGAGCAGCTTTTTAAGGG
C-MYC forward primer	TGGAGGGTTGCGGGTGTCGCGGTGGCGGAGGTGGCGAGCAGAAGCTGATCAGCGAGGAGGACCTGTAGCACAGCAAGATCTAGGATCC
C-MYC reverse primer	GGATCCTAGATCTTGCTGTGCTACAGGTCCTCCTCGCTGATCAGCTTCTGCTCGCCACCTCCGCCACCGCGACACCCGCAACCCTCCA
N-FLAG forward primer	GGCCTGGGGGGACCCCATGGATGGACTACAAGGACGACGACGACAAGGGTGGCGGAGGTGGCCCAGCCCCCCCTCCTCCACT
N-FLAG reverse primer	AGTGGAGGAGGGGGGGCTGGGCCACCTCCGCCACCCTTGTCGTCGTCGTCCTTGTAGTCCATCCATGGGGTCCCCCCAGGCC

Table 2. Hematoxylin and Eosin tissue staining procedure
5 µm thick sections of colon tissue were dried onto microslides and subjected to the following H&E staining procedure.

Step	Reagent	Time (Min:Sec)
1	Clear-Rite (Thermo Scientific)	3:00
2	Clear-Rite (Thermo Scientific)	3:00
3	Clear-Rite (Thermo Scientific)	3:00
4	100% EtOH	1:00
5	100% EtOH	1:00
6	95% EtOH	1:00
7	Distilled Water	1:00
8	Hematoxylin	1:30
9	Distilled Water	1:00
10	Clarifier (Thermo Scientific)	0:50
11	Distilled Water	1:00
12	Bluing Reagent (Thermo Scientific)	1:00
13	Distilled Water	1:00
14	95% EtOH	0:30
15	Eosin	1:30
16	100% EtOH	1:00
17	100% EtOH	1:00
18	Clear-Rite (Thermo Scientific)	1:00
19	Clear-Rite (Thermo Scientific)	1:00
20	Clear-Rite (Thermo Scientific)	1:00

Figures

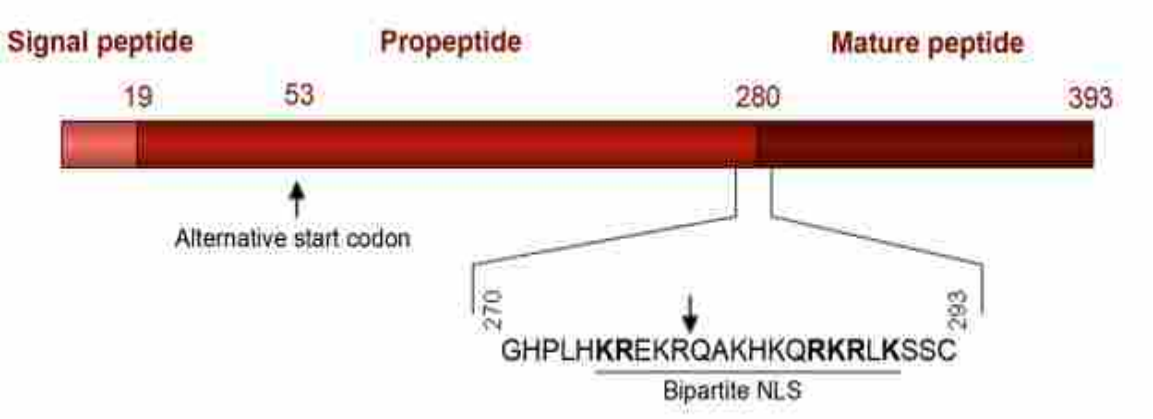

Figure 1. Schematic of the BMP2 preproprotein
Map of the rat BMP2 preproprotein showing the signal peptide, propeptide, and mature peptide. The amino acid sequence and location of the bipartite NLS is indicated, and the site of proteolytic cleavage is marked by an arrow. The downstream alternative start codon used for translating nBMP2 is also indicated.

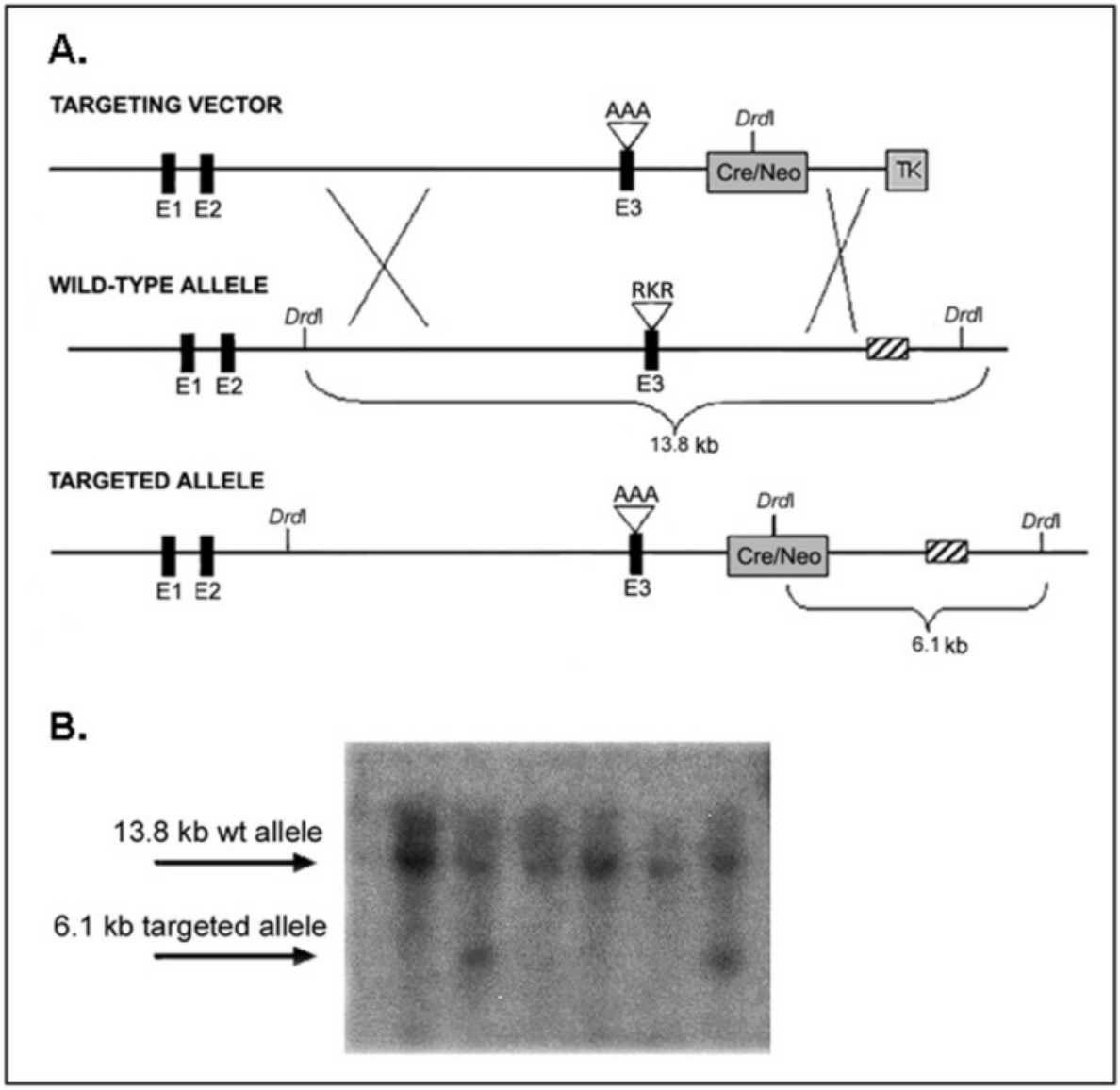

Figure 2. Targeted mutation of nBmp2 in mouse model
(A) A mutation was introduced at the NLS site (RKR to AAA) to prevent nuclear localization of nBMP2. (B) Successful recombination of the targeted allele is shown by the 6.1 kb band in a Southern blot. Stem cells with the selected mutation were implanted in a host embryo and transferred to a surrogate mother. Heterozygous mutant mice (nBmp2NLS^{tm}) were then bred to homozygosity.

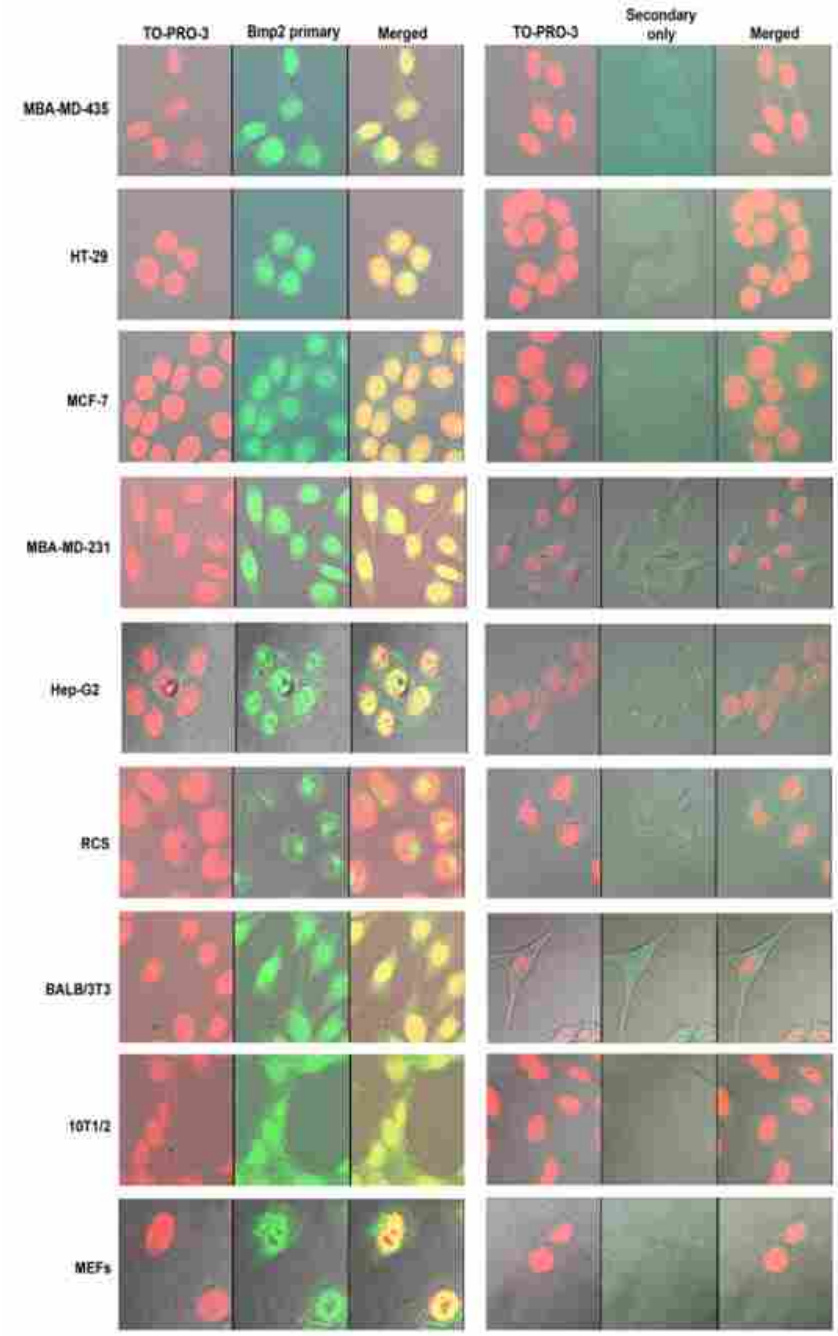

Figure 3. **nBMP2 is endogenously expressed in several cancer cell lines**
Cells were cultured and immunostained using an anti-BMP2 antibody followed by an Alexa Fluor 488-tagged secondary antibody (green). Nuclei were stained with TO-PRO-3 (red), and cells were examined by laser confocal microscopy. Many cell cultures contained cells with strong nuclear localization of BMP2. Staining with only the secondary antibody gave little or no signal, as indicated by the panels on the right-hand side of the figure.

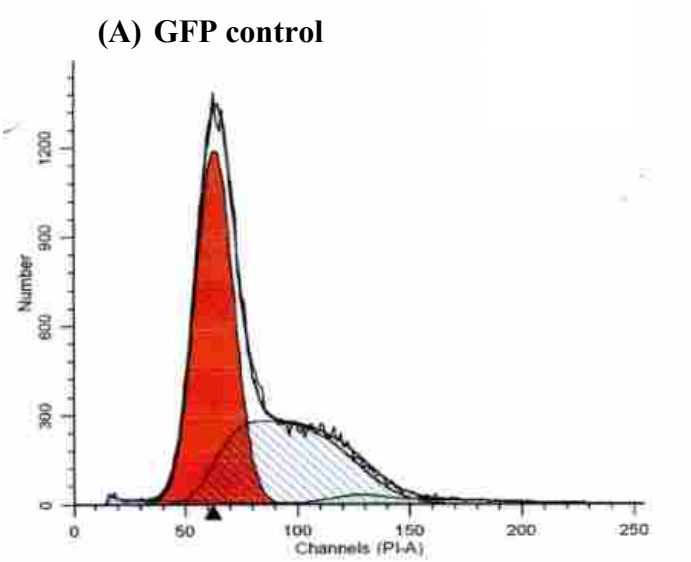

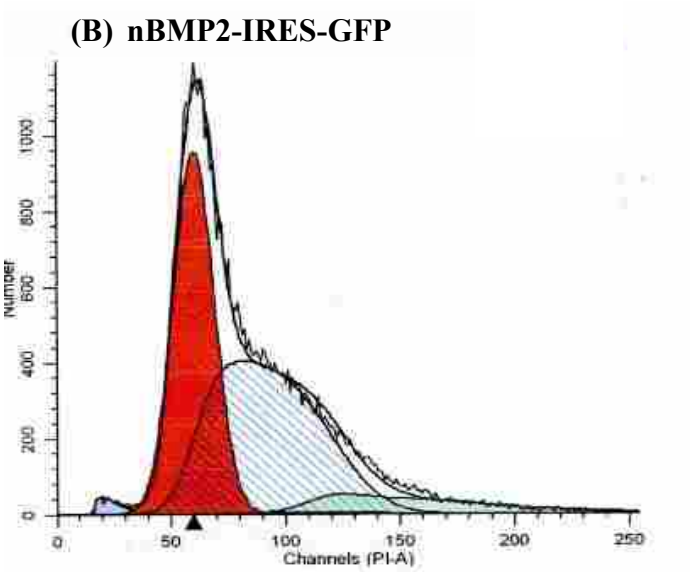

Figure 4. nBMP2 increases the fraction of cells in S-phase of the cell cycle
Modfit graphs of a representative cell cycle analysis experiment from HEK293 cells transfected with (A) GFP control plasmid or (B) nBMP2-IRES-GFP plasmid. Area under the curve in red represents amount of cells in G1 phase, the area under the blue-striped curve represents percentage of cells in S-phase of the cell cycle, and green represents cell aggregates. GFP+ cells were gated and the percentage of cells in each phase of the cell cycle was analyzed using Modfit LT software.

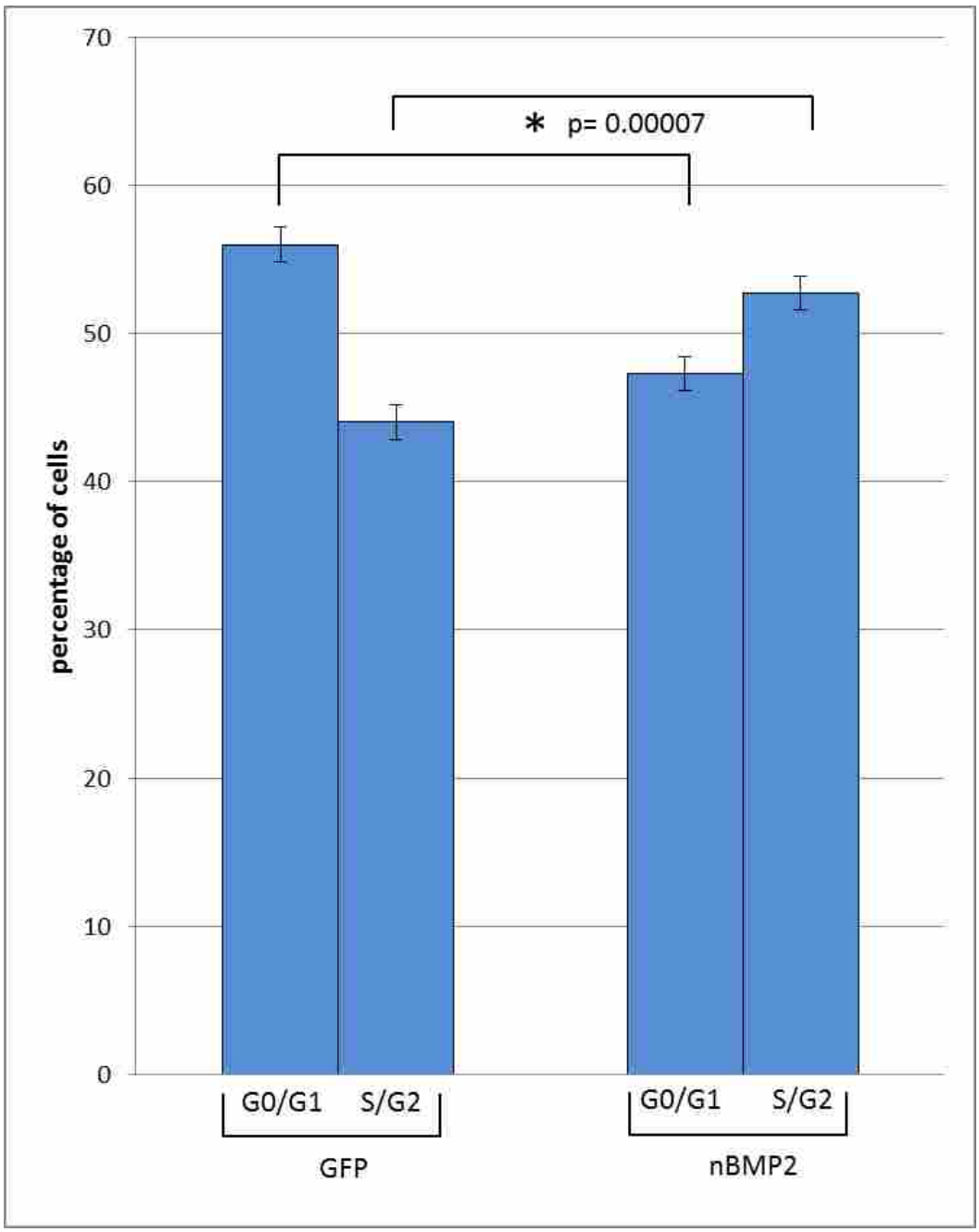

Figure 5. Overexpression of nBMP2 promotes cell cycle progression in HEK293 cell line
HEK293 cells were transfected with either a control GFP plasmid or an nBMP2-IRES-GFP plasmid and fixed with formaldehyde. After permeabilizing the cells with ethanol, cells were stained with propidium iodide. Samples were analyzed by flow cytometry with the GFP+ cell population gated to isolate transfected cells for analysis. Cell cycle was analyzed using Modfit LT software. Results are from three independent experiments, each performed in triplicate with bars indicating standard error.

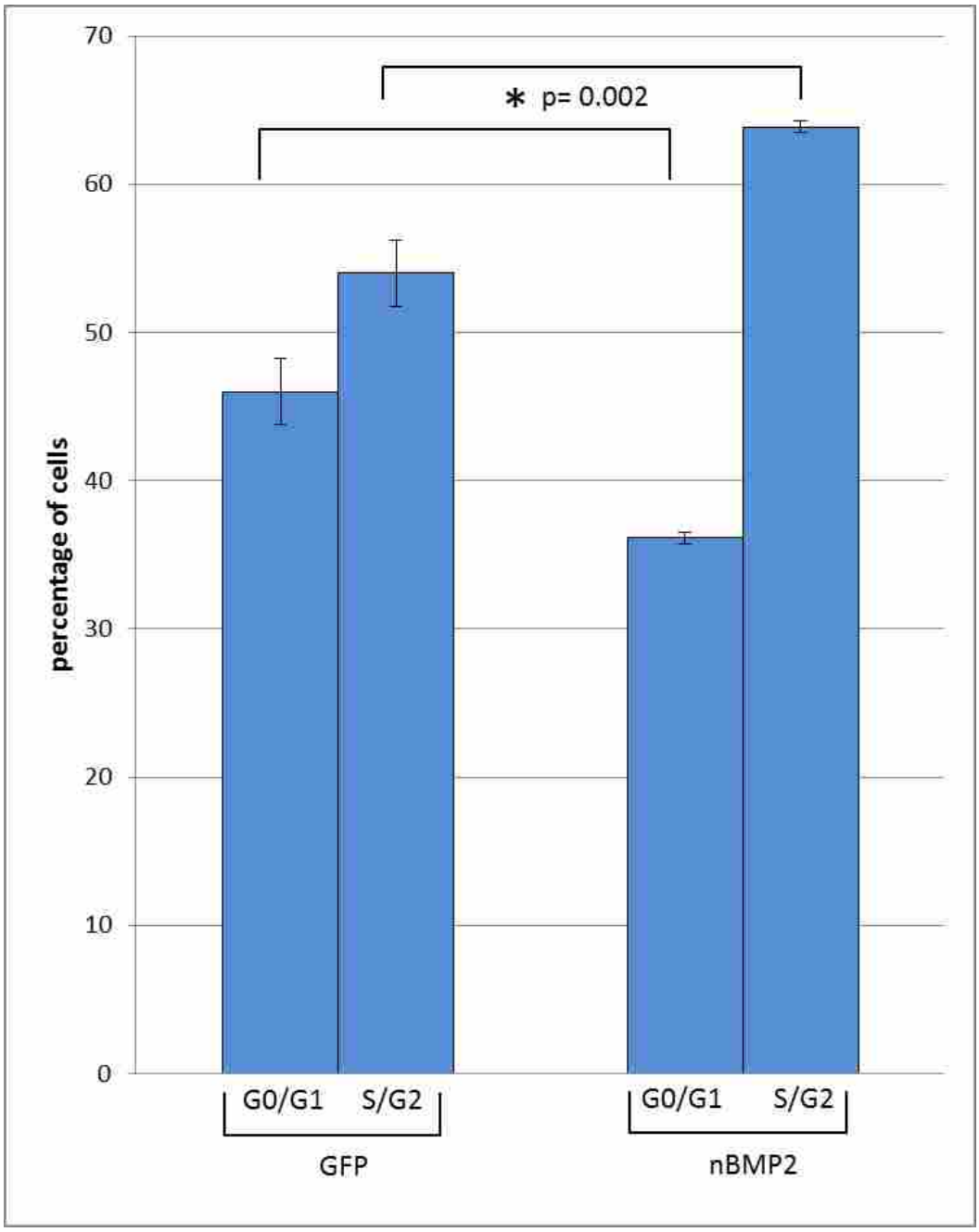

Figure 6. Overexpression of nBMP2 promotes cell cycle progression in HT29 cell line
HT29 cells were transfected with either a control GFP plasmid or an nBMP2-IRES-GFP plasmid and fixed with formaldehyde. After permeabilizing the cells with ethanol, cells were stained with propidium iodide. Samples were analyzed by flow cytometry with the GFP+ cell population gated to isolate transfected cells for analysis. Cell cycle was analyzed using Modfit LT software. Results are from three independent experiments, each performed in triplicate with bars indicating standard error.

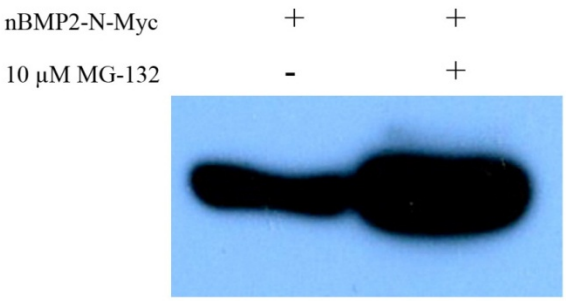

Figure 7. nBMP2 is actively degraded by the proteasome
HEK293 cells were transfected with nBMP2-N-MYC plasmid, with or without 10 μM MG132 proteasome inhibitor. Cell lysate was harvested and analyzed by western blot, probed with anti-Myc antibody.

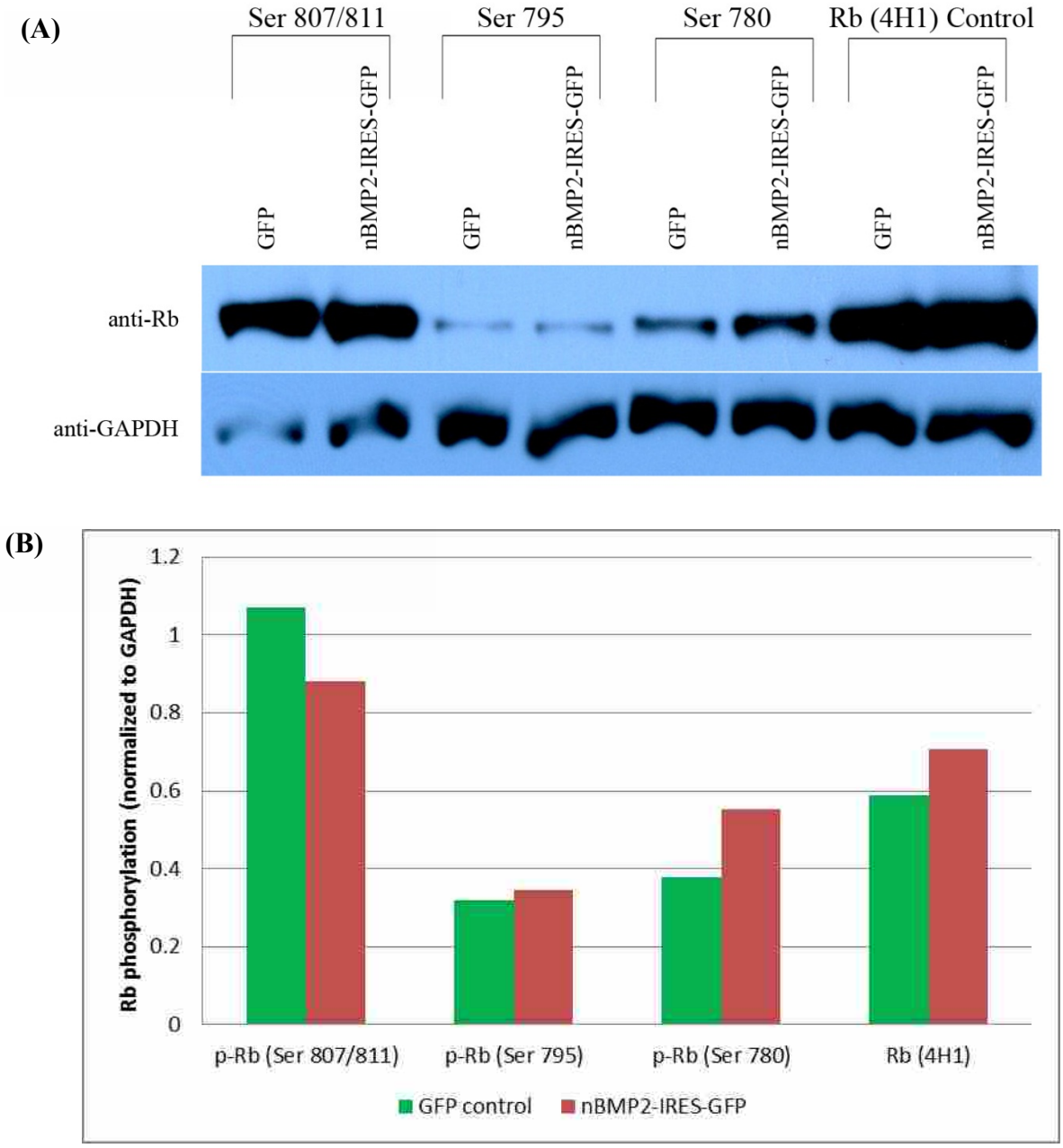

Figure 8. nBMP2 does not induce hyperphosphorylation of Rb
(A) HEK293 cells were transfected with either GFP control plasmid or nBMP2-IRES-GFP, and lysate was analyzed by western blot using several antibodies for specific phosphorylation sites on Rb. (B) A graphical representation of immunoblots with band intensity normalized to GAPDH.

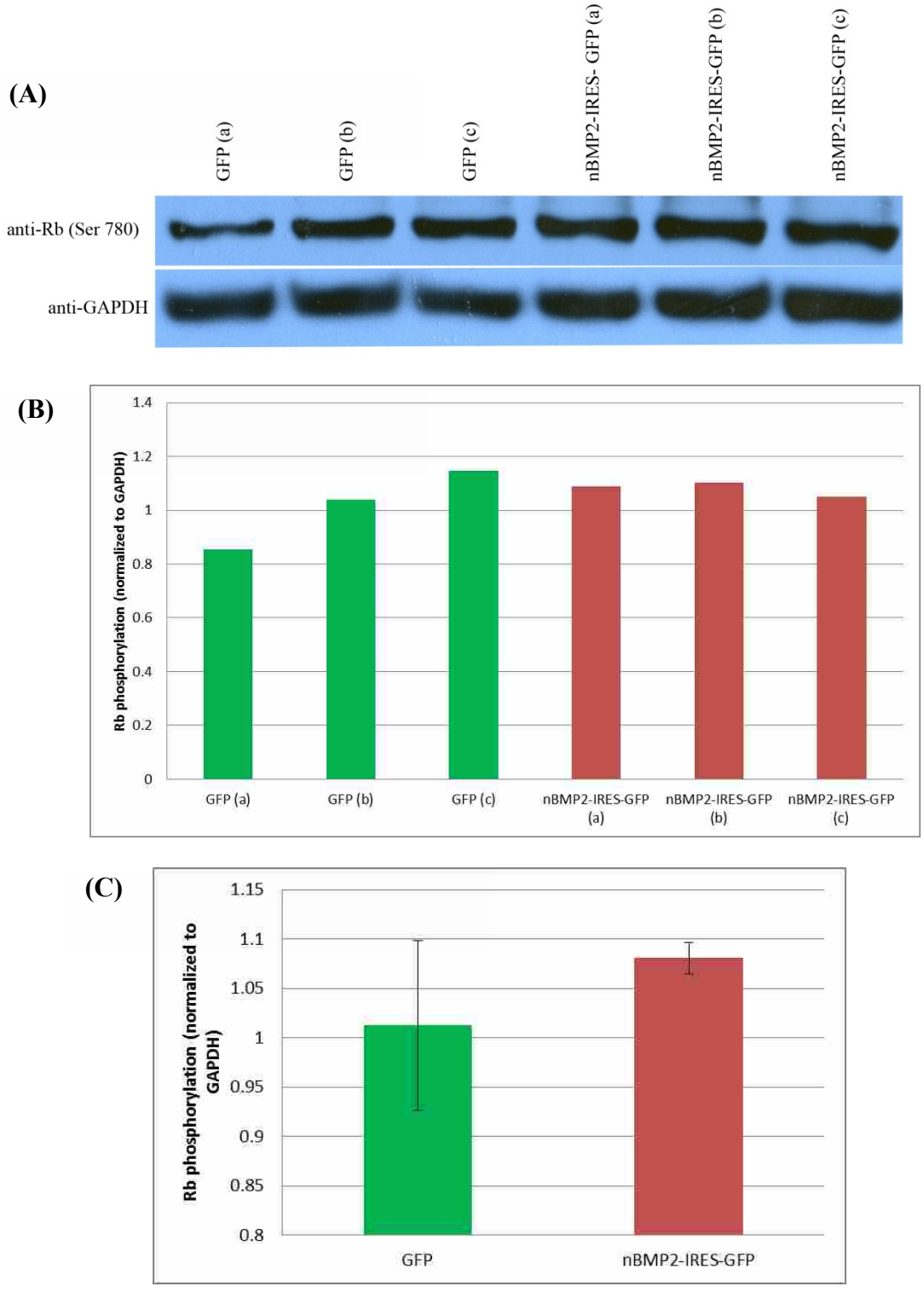

Figure 9. Rb (Ser 780) is not hyperphosphorylated with nBMP2 overexpression
HEK293 cells were transfected with either GFP control plasmid or nBMP2-IRES-GFP, and lysate was analyzed by western blot using Rb (Ser780) antibody (A). Phosphorylation levels were normalized to GAPDH (B) and triplicate samples were averaged (C) with bars indicating standard error.

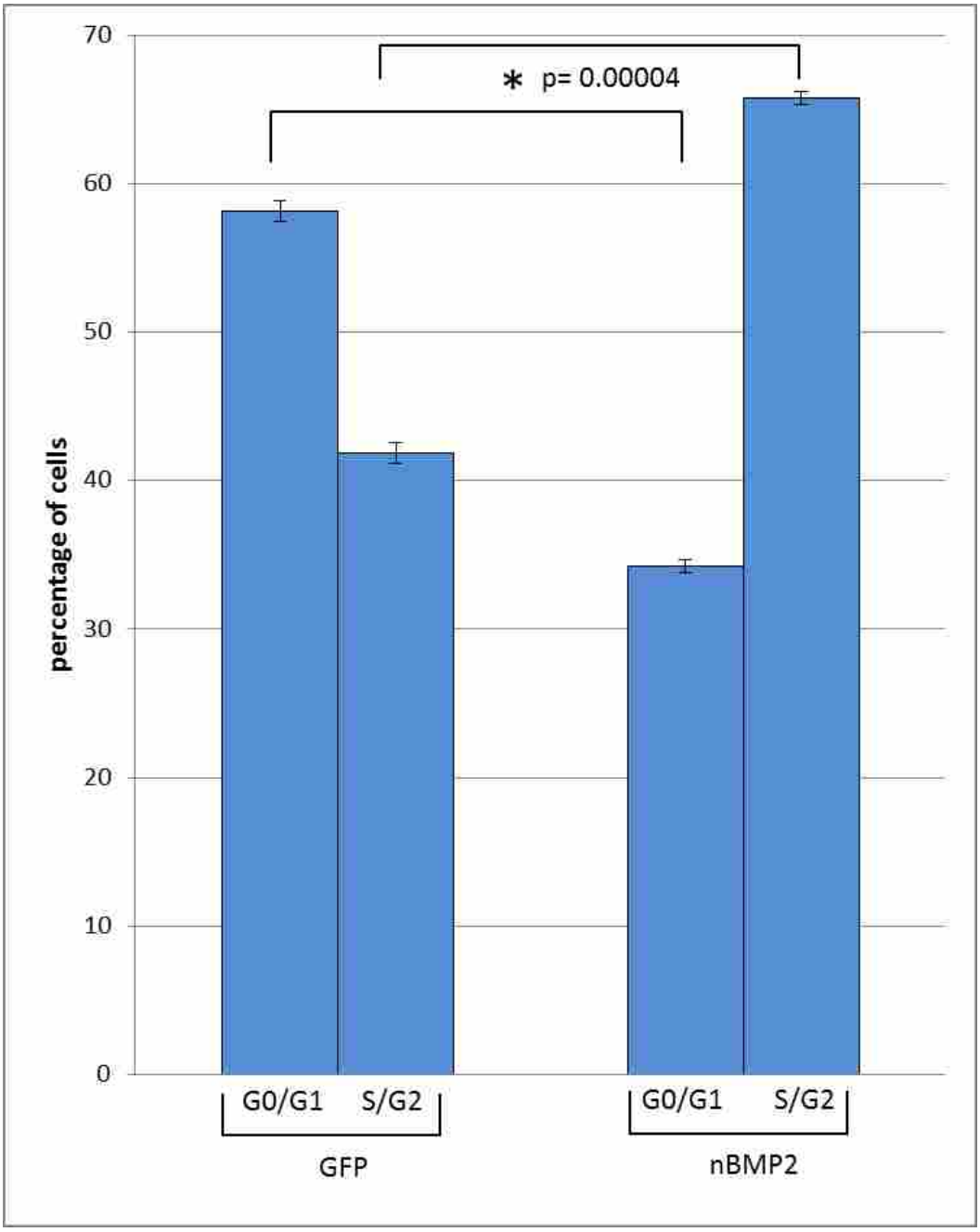

Figure 10. nBMP2-C-GFP fusion protein promotes cell cycle progression
HEK293 cells were transfected with either a control GFP plasmid or an nBMP2-C-GFP plasmid and fixed with formaldehyde. After permeabilizing the cells with ethanol, cells were stained with propidium iodide. Samples were analyzed by flow cytometry with the GFP+ cell population gated to isolate transfected cells for analysis. Cell cycle was analyzed using Modfit LT software. Results are from one independent experiment performed in triplicate with bars indicating standard error.

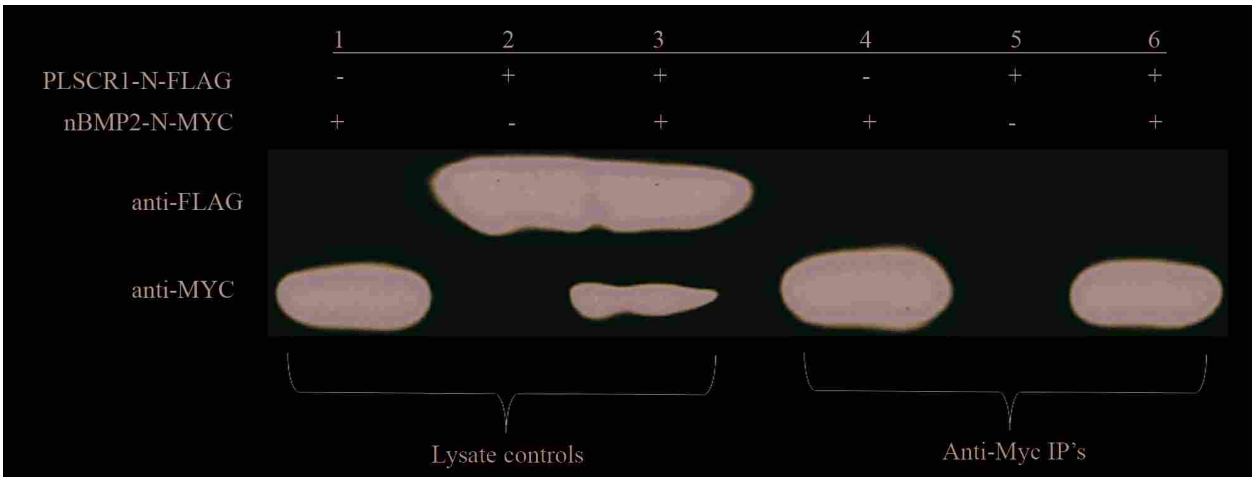

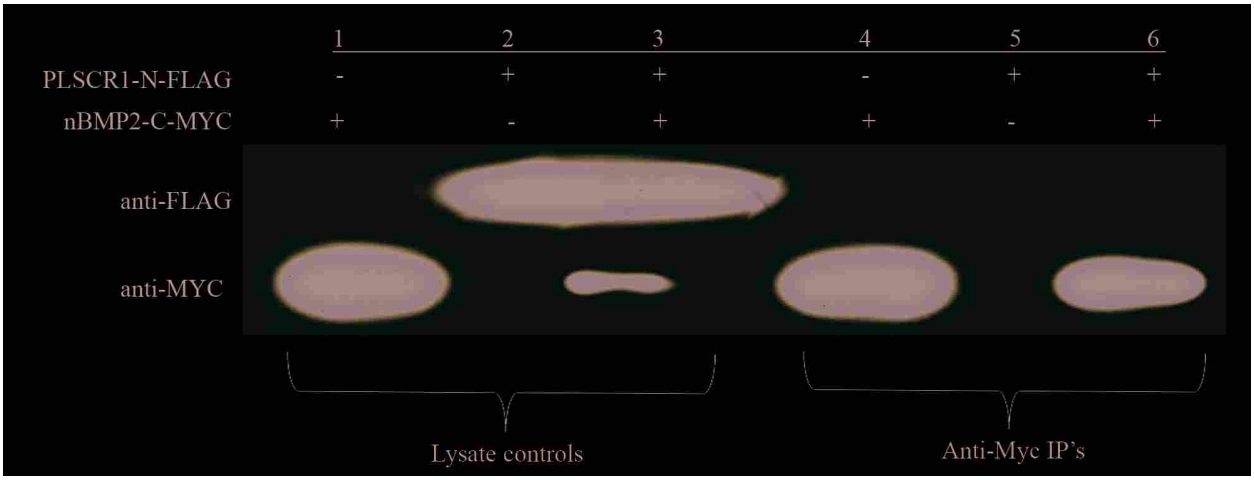

Figure 11. nBMP2 and PLSCR1 show no interaction by co-immunoprecipitation
Western blots for (A) nBMP2-N-MYC and (B) nBMP2-C-MYC with PLSCR-1. Lysate controls show that transfection was successful and proteins are expressed (lanes 1-3). Lysate was pulled down with Myc-sepharose conjugated beads (lanes 4-6). Myc-IP's show no interaction between nBMP2 and PLSCR-1 (lane 6).

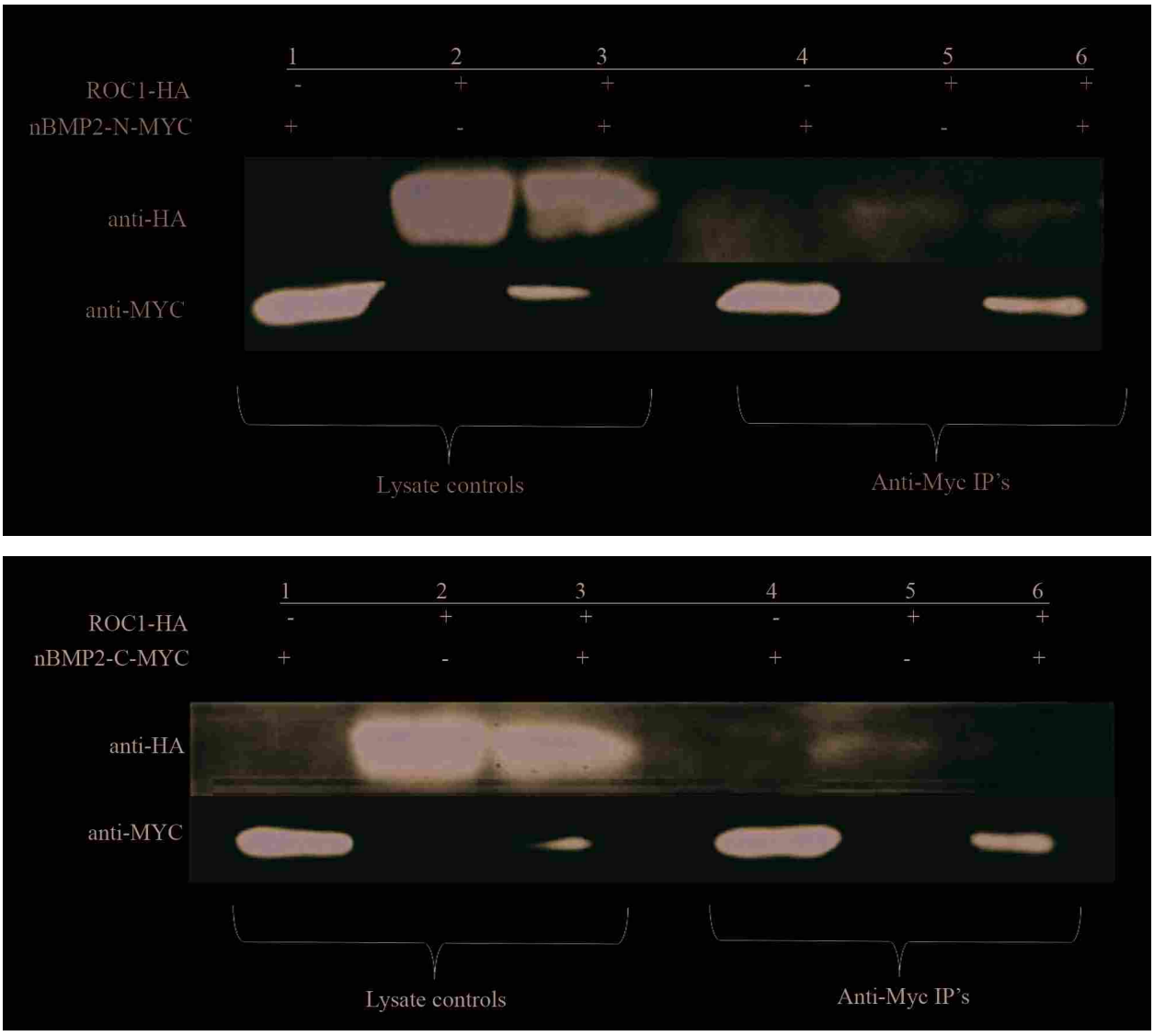

Figure 12. nBMP2 and ROC1 interaction was not confirmed by co-immunopreciptiation Western blots for (A) nBMP2-N-MYC and (B) nBMP2-C-MYC with ROC1-HA. Lysate controls show that transfection was successful and proteins are expressed (lanes 1-3). Lysate was pulled down with Myc-sepharose conjugated beads (lanes 4-6). Myc-IP's show that ROC1 may be present in lane 6, but there appears to be non-specific binding of ROC1-HA to the beads as observed in lane 5, so we cannot confirm the interaction between nBMP2 and ROC1.

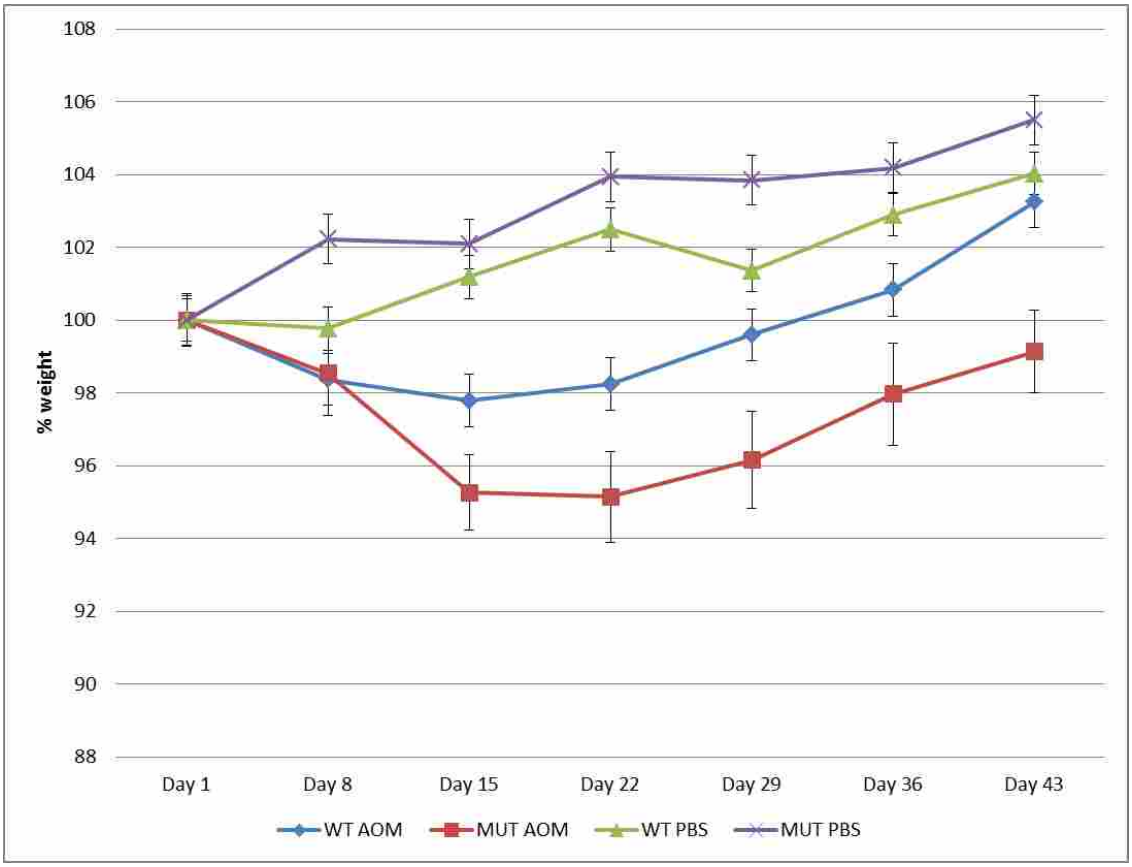

Figure 13. AOM treated mice display decreased weight gain in 6-week study
Mice were weighed weekly for the duration of the 6-week study. Mice injected with AOM suffered greater weight loss compared to the PBS control mice. Also, AOM treated mutant mice displayed a trend of greater decrease in weight compared to AOM treated wild type mice ($p=0.19$ on Day 43). WT AOM n=8, MUT AOM n=6, WT PBS n=5, MUT PBS n=4. Bars indicate standard error.

(A)

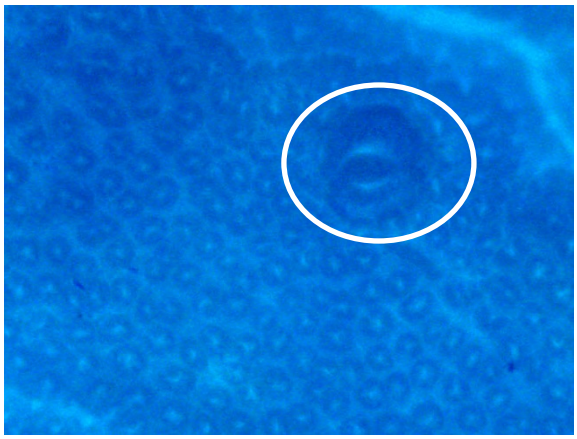

(B)

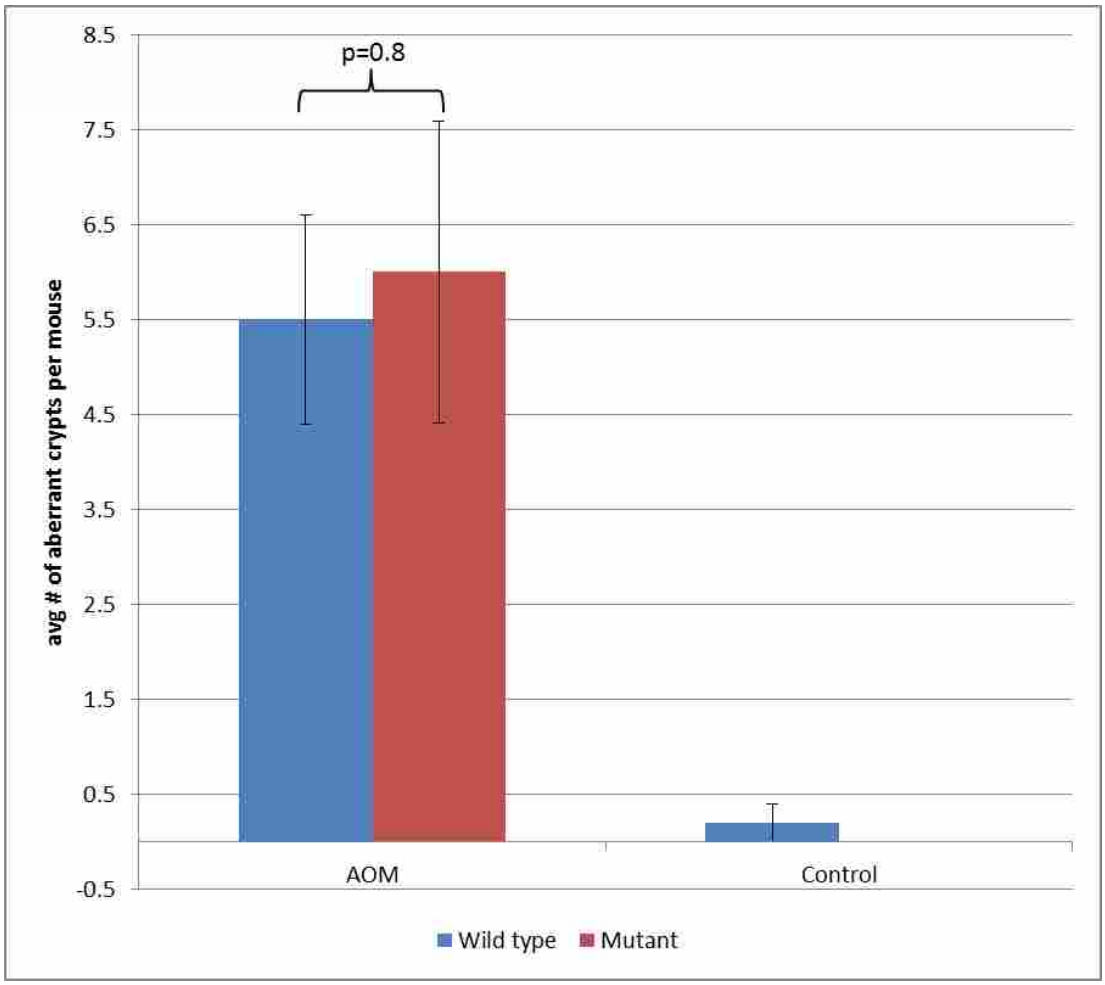

Figure 14. Aberrant crypt counts for 6-week study
Mice were treated with 3 weekly injections of AOM and euthanized 3 weeks after the final injection. (A) Image of two adjacent (circled) aberrant crypts which are identified by dark, thickened borders and enlarged luminal openings following methylene blue stain. (B) Aberrant crypts were quantified and averaged. WT AOM n=8, MUT AOM n=6, WT PBS n=5, MUT PBS n=4. Bars indicate standard error.

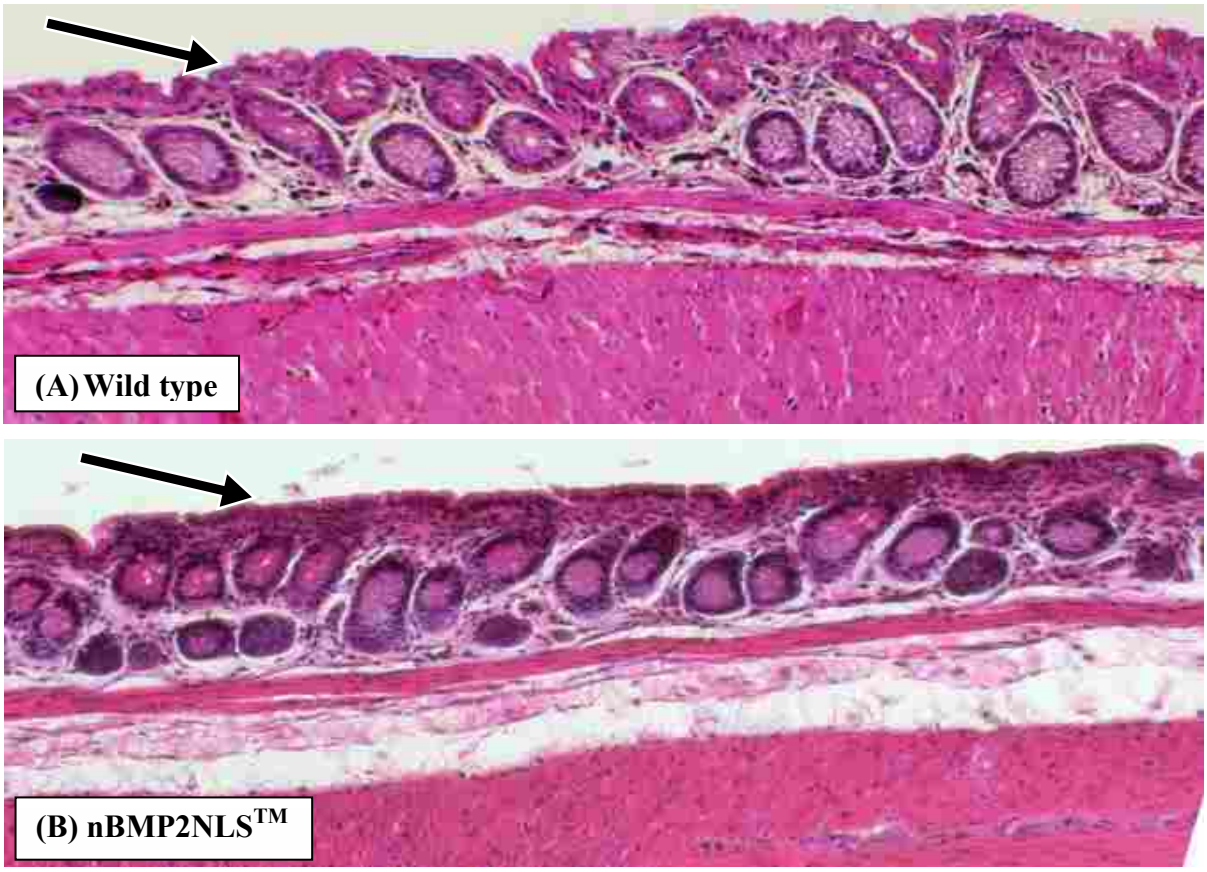

Figure 15. H&E stain of AOM treated nBmp2NLS^{tm} mice shows dysplasia in 6-week study
H&E stain of 5 µm-thick longitudinal sections of AOM treated mouse colons from (A) wild type mice and (B) nBmp2NLS^{tm} mice. Arrow points to layer of tissue showing (A) typical monolayer of nuclei and (B) abnormal amounts of nuclei indicating dysplasia.

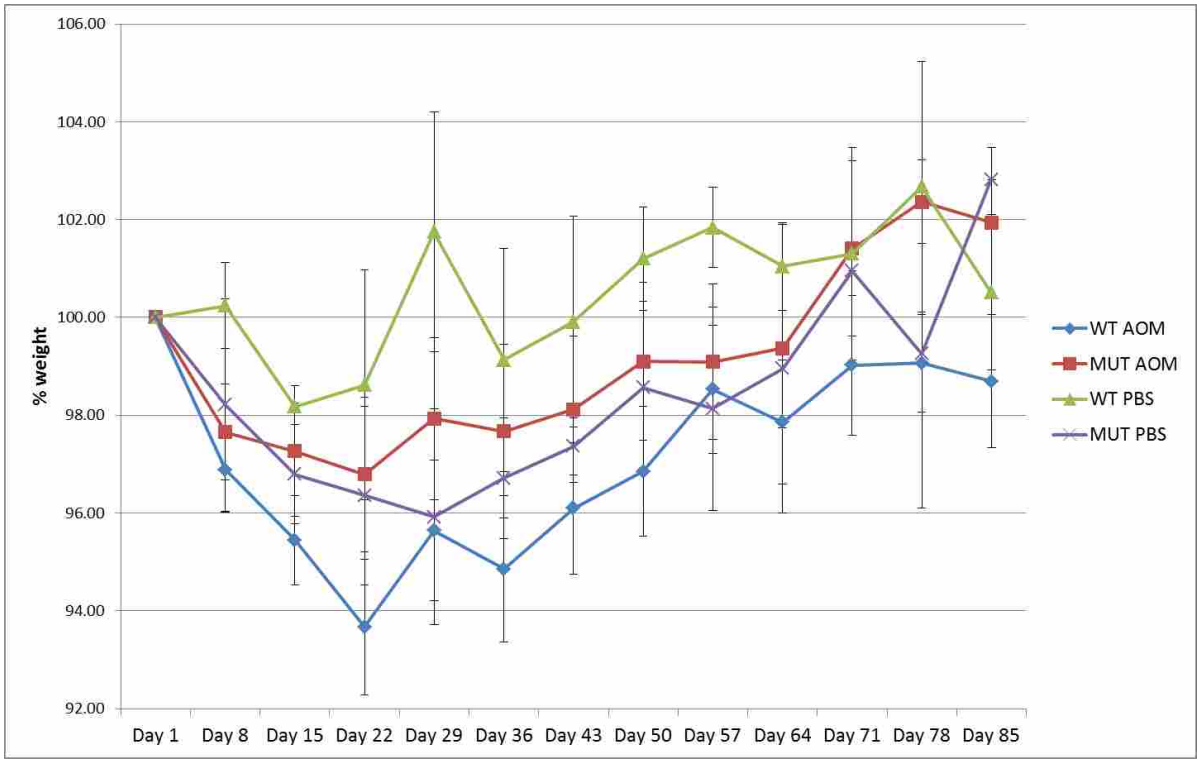

Figure 16. No significant differences in weight change between mice in 12-week study
No significant differences in percent of original body weight were observed between nBmp2NLS^{tm} and wild type mice after AOM treatment in the 12-week study. WT AOM n=8, MUT AOM n=8, WT PBS n=2, MUT PBS n=2. Bars indicate standard error.

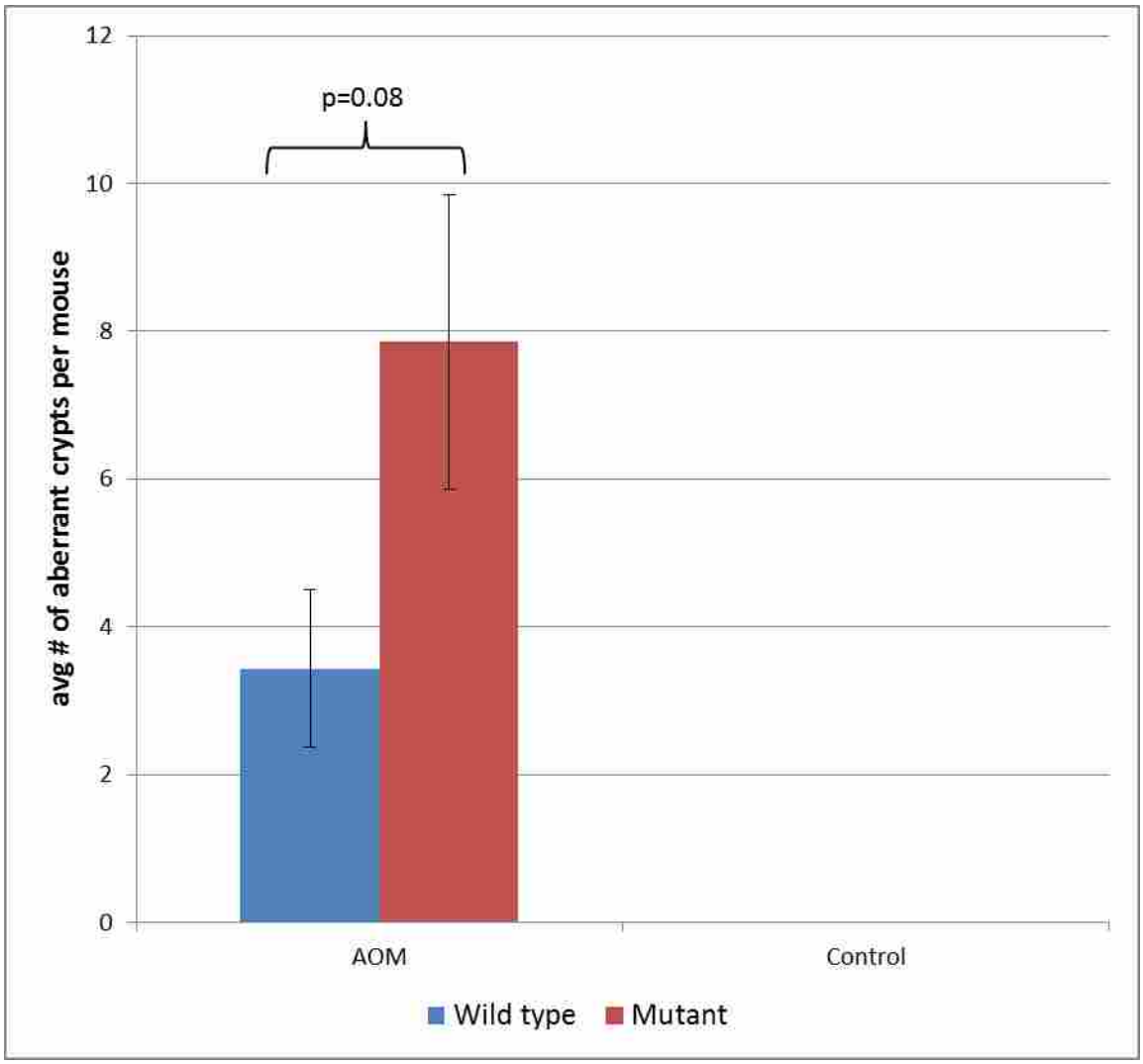

Figure 17. Trend shows more aberrant crypts in nBmp2NLS^{tm} mice than in wild type mice in 12-week study

Mice were treated with 3 weekly injections of AOM and euthanized 10 weeks after the final injection. Tissues were stained with methylene blue and aberrant crypts were quantified. No aberrant crypts were found in PBS control tissues. WT AOM n=8, MUT AOM n=8, WT PBS n=2, MUT PBS n=2. Bars indicate standard error.

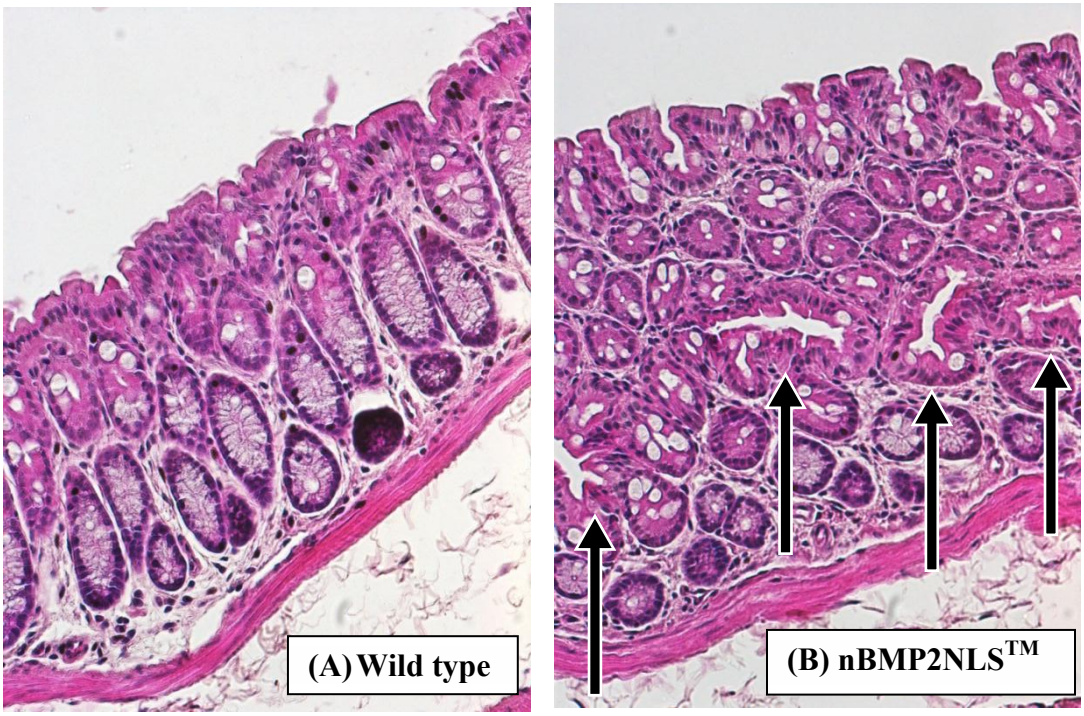

Figure 18. H&E stain shows aberrant crypts in nBmp2NLS^{tm} mice in 12-week study
H&E stain of 5 µm-thick longitudinal sections of AOM treated mouse colons from wild type (A) and nBmp2NLS^{tm} (B) mice. Four aberrant crypts are indicated by arrows in nBmp2NLS^{tm} mice (B).

References

1. Urist, M.R., *Bone: Formation by Autoinduction.* Science, 1965. **150**(3698): p. 893-899.
2. Shu, B., et al., *BMP2, but not BMP4, is crucial for chondrocyte proliferation and maturation during endochondral bone development.* Journal Of Cell Science, 2011. **124**(Pt 20): p. 3428-3440.
3. Zhang, H. and A. Bradley, *Mice deficient for BMP2 are nonviable and have defects in amnion/chorion and cardiac development.* Development (Cambridge, England), 1996. **122**(10): p. 2977-2986.
4. Langenfeld, E.M., et al., *Expression of bone morphogenetic proteins in human lung carcinomas.* Ann Thorac Surg, 2005. **80**(3): p. 1028-32.
5. Raida, M., et al., *Bone morphogenetic protein 2 (BMP-2) and induction of tumor angiogenesis.* J Cancer Res Clin Oncol, 2005. **131**(11): p. 741-50.
6. Kawamura, C., M. Kizaki, and Y. Ikeda, *Bone morphogenetic protein (BMP)-2 induces apoptosis in human myeloma cells.* Leuk Lymphoma, 2002. **43**(3): p. 635-9.
7. Chen, A., et al., *Inhibitory effect of BMP-2 on the proliferation of breast cancer cells.* Molecular Medicine Reports, 2012. **6**(3): p. 615-620.
8. Wang, L., et al., *BMP-2 inhibits tumor growth of human renal cell carcinoma and induces bone formation.* International Journal Of Cancer. Journal International Du Cancer, 2012. **131**(8): p. 1941-1950.
9. Jin, H., et al., *BMP2 promotes migration and invasion of breast cancer cells via cytoskeletal reorganization and adhesion decrease: an AFM investigation.* Applied Microbiology And Biotechnology, 2012. **93**(4): p. 1715-1723.
10. Kim, M. and S. Choe, *BMPs and their clinical potentials.* BMB Rep, 2011. **44**(10): p. 619-34.
11. Felin, J.E., et al., *Nuclear variants of bone morphogenetic proteins.* BMC Cell Biology, 2010. **11**: p. 20-20.
12. Odermatt, A., et al., *Mutations in the gene-encoding SERCA1, the fast-twitch skeletal muscle sarcoplasmic reticulum Ca2+ ATPase, are associated with Brody disease.* Nature Genetics, 1996. **14**(2): p. 191-194.
13. Odermatt, A., et al., *The mutation of Pro789 to Leu reduces the activity of the fast-twitch skeletal muscle sarco(endo)plasmic reticulum Ca2+ ATPase (SERCA1) and is associated with Brody disease.* Human Genetics, 2000. **106**(5): p. 482-491.
14. Fitzjohn, S.M. and G.L. Collingridge, *Calcium stores and synaptic plasticity.* Cell Calcium, 2002. **32**(5-6): p. 405-411.
15. Straub, S.V. and M.T. Nelson, *Astrocytic calcium signaling: the information currency coupling neuronal activity to the cerebral microcirculation.* Trends In Cardiovascular Medicine, 2007. **17**(6): p. 183-190.
16. Malenka, R.C., et al., *Postsynaptic calcium is sufficient for potentiation of hippocampal synaptic transmission.* Science (New York, N.Y.), 1988. **242**(4875): p. 81-84.
17. Myoga, M.H. and W.G. Regehr, *Calcium microdomains near R-type calcium channels control the induction of presynaptic long-term potentiation at parallel fiber to purkinje cell synapses.* The Journal Of Neuroscience: The Official Journal Of The Society For Neuroscience, 2011. **31**(14): p. 5235-5243.

18. Vargas, R., F. Cifuentes, and M.A. Morales, *Role of presynaptic and postsynaptic IP3-dependent intracellular calcium release in long-term potentiation in sympathetic ganglion of the rat.* Synapse (New York, N.Y.), 2011. **65**(5): p. 441-448.
19. Pande, G., N.A. Kumar, and P.S. Manogaran, *Flow cytometric study of changes in the intracellular free calcium during the cell cycle.* Cytometry, 1996. **24**(1): p. 55-63.
20. Weinberg, R.A., *The retinoblastoma protein and cell cycle control.* Cell, 1995. **81**(3): p. 323-330.
21. Sherr, C.J., *Cancer cell cycles.* Science (New York, N.Y.), 1996. **274**(5293): p. 1672-1677.
22. Knudsen, E.S. and J.Y. Wang, *Dual mechanisms for the inhibition of E2F binding to RB by cyclin-dependent kinase-mediated RB phosphorylation.* Molecular And Cellular Biology, 1997. **17**(10): p. 5771-5783.
23. Sherr, C.J. and J.M. Roberts, *CDK inhibitors: positive and negative regulators of G1-phase progression.* Genes & Development, 1999. **13**(12): p. 1501-1512.
24. Nakayama, K.I. and K. Nakayama, *Regulation of the cell cycle by SCF-type ubiquitin ligases.* Seminars In Cell & Developmental Biology, 2005. **16**(3): p. 323-333.
25. Wei, D. and Y. Sun, *Small RING Finger Proteins RBX1 and RBX2 of SCF E3 Ubiquitin Ligases: The Role in Cancer and as Cancer Targets.* Genes Cancer, 2010. **1**(7): p. 700-7.
26. Hanahan, D. and R.A. Weinberg, *Hallmarks of cancer: the next generation.* Cell, 2011. **144**(5): p. 646-674.
27. Monteith, G.R., et al., *Calcium and cancer: targeting Ca2+ transport.* Nature Reviews. Cancer, 2007. **7**(7): p. 519-530.
28. Chung, F.Y., et al., *Sarco/endoplasmic reticulum calcium-ATPase 2 expression as a tumor marker in colorectal cancer.* Am J Surg Pathol, 2006. **30**(8): p. 969-74.
29. Mayo, J.L., *Characterization of a Novel Nuclear Variant of Bmp2 and Coordinate Regulation of Col11a2 and Col27a1 by the Transcription Factor Lc-Maf.* BYU Microbiology and Molecular Biology, 2007.
30. Zhou, Q., et al., *Phospholipid scramblase 1 binds to the promoter region of the inositol 1,4,5-triphosphate receptor type 1 gene to enhance its expression.* The Journal Of Biological Chemistry, 2005. **280**(41): p. 35062-35068.
31. Bhatia, V., M.K. Saini, and M. Falzon, *Nuclear PTHrP targeting regulates PTHrP secretion and enhances LoVo cell growth and survival.* Regulatory Peptides, 2009. **158**(1-3): p. 149-155.
32. Bonnet, H., et al., *Fibroblast growth factor-2 binds to the regulatory beta subunit of CK2 and directly stimulates CK2 activity toward nucleolin.* The Journal Of Biological Chemistry, 1996. **271**(40): p. 24781-24787.
33. Kiefer, P., et al., *Competition between nuclear localization and secretory signals determines the subcellular fate of a single CUG-initiated form of FGF3.* The EMBO Journal, 1994. **13**(17): p. 4126-4136.
34. Abdel-Samad, R., et al., *MiniSOX9, a dominant-negative variant in colon cancer cells.* Oncogene, 2011. **30**(22): p. 2493-2503.